Multidisciplinary Optimization of Shoe Midsole Structures using Tetrahedral Mesh Generation and Swarm Intelligence

Maksudul Alam

A Thesis

in

The Department

of

Mechanical, Industrial

and

Aerospace Engineering

Presented in Partial Fulfillment of the Requirements

for the Degree of Master of Applied Science (Mechanical Engineering) at

Concordia University

Montreal, Quebec, Canada

May 2023

CONCORDIA UNIVERSITY

School of Graduate Studies

This is to certify that the thesis is prepared

By: Maksudul Alam

Entitled: Multidisciplinary Optimization of Shoe Midsole Structures using Tetrahedral Mesh Generation and Swarm Intelligence

and submitted in partial fulfillment of the requirements for the degree of

Master of Applied Science (Mechanical Engineering)

complies with the regulations of the University and meets the accepted standards with respect to originality and quality.

Signed by the final Examining Committee:

_____ Chair

Dr. Chevy Chen

_____ Examiner

Dr. Chevy Chen

_____ Examiner

Dr. Hang Xu

_____ Supervisor

Dr. Tsz Ho Kwok

Approved by _____

Dr. Martin D. Pugh, Chair of Department or Graduate Program Director

5/10/2023 _____

Date *Dr. Mourad Debbabi, Dean of Faculty*

Abstract

Multidisciplinary Optimization of Shoe Midsole Structures using Tetrahedral Mesh Generation and Swarm Intelligence

by Maksudul Alam

Creating functional midsoles for shoes is a challenging task that involves considering different aspects such as stability, comfort, manufacturability, and aesthetics. No single approach exists to design a midsole that meets all these objectives effectively. Therefore, this study aims to introduce a multidisciplinary optimization method to develop custom shoe midsole structures. The proposed approach involves utilizing tetrahedral mesh generation to generate diverse structures and leveraging swarm intelligence to search for optimal designs. Tetrahedral mesh generation is used to create midsole structures because tetrahedral structures are renowned for their exceptional strength. Additionally, tetrahedral mesh generation is a well-established tool that provides the added advantage of fully automatic construction for complex-shaped midsoles. By adjusting the mesh generation parameters, a wide range of solutions can be generated that meet multiple objectives. To enhance the swarm's exploration of the design space and discover more local optima, a new swarm behavior is developed that promotes diversity. Furthermore, a quantitative measurement tool is created to evaluate various objectives. In order to test the effectiveness of the generative approach, the midsoles obtained from the design exploration are analyzed that performed the best and the worst in relation to each objective. The findings revealed a substantial difference between them, with scores differing by two to four times. Additionally, when compared to other lattice structures, the tetrahedral midsole structure created by the proposed method demonstrated superior compliance with the foot and better redistribution of plantar stress. This makes it an ideal candidate for use in shoe midsoles. The multidisciplinary optimization technique

proposed here is a valuable resource for engineers and designers in the footwear industry, allowing them to develop high-performance midsole structures that meet the needs of both consumers and athletes. Furthermore, this method can be applied to optimize other complex structures in various industries, such as civil, automotive, and aerospace engineering.

Acknowledgements

All praise and thanks to the Almighty, by whose blessings my research work was completed successfully. I would like to express my sincere gratitude to my research supervisor, Dr. Tsz Ho Kwok, for allowing me to do research and granting me valuable guidance throughout this research. His incredible patience, sincere motivation, and immense knowledge inspired me enormously. It was a great opportunity and an honor to work and study under his supervision. I could not have imagined having a better advisor and mentor for my MASc study. I am incredibly grateful to my family, friends, and research colleagues, Christopher Danny-Matte, Eder da Silva Sales, Christopher Richard, Shiva Shokri, and especially Ankhy Sultana, for their sincere help. my appreciation to the committee members, Dr. Chevy Chen and Dr. Hang Xu, and my beloved Concordia University. Thanks to all who supported me.

Contents

List of Figures

List of Tables

List of Abbreviations

FFF	Fused Filament Fabrication
PLA	Polylactic Acid
TPU	Thermoplastic Polyurethane
PSO	Particle Swarm Optimization
ρ_{max}	Maximum Radius-to-Edge ratio
φ_{min}	Minimum Dihedral Angle
V_{max}	Maximum Volume of tetrahedrons
S_{max}	Maximum Stress
T_{max}	Maximum Temperature

1 Introduction

Traditional production methods have gradually changed through digitization. As a result of a significant improvement in living standards, people are now paying much more attention to their health issues. Technological progress has made it feasible to create customized footwear that meets specific mechanical, thermal, and aesthetic requirements. As consumer interest in footwear has expanded beyond durability and appearance to include functional modifications tailored to their individual characteristics, the anticipated domain in this analysis is the shoe midsole, which is considered the most essential part of a shoe.

1.1 Motivation

Footwear serves a physiological function for a human being. Wearing appropriate footwear is one of the primary means of maintaining a suitable environment to protect the feet, which bear the weight of the body and are exposed to daily stress. The sole of a shoe is comprised of three parts, including the insole, midsole, and outsole, with the midsole playing a critical role in stabilizing the body, absorbing shocks and energy, and providing comfort (see Fig. 1.1). In addition to the necessary stiffness, the midsole also has to have a certain amount of elasticity and flexibility; otherwise, it will result in high plantar pressure. High peak plantar pressure is one of the major reasons for painful forefoot syndromes. It can lead to foot ulcers, which are a common complication of diabetes. These ulcers can occur due to the breakdown of skin and tissue caused by excessive pressure on the foot. Infections can result from foot ulcers, which can be challenging to treat. High plantar pressure can exacerbate diabetes's poor blood circulation, which makes it more difficult for sores on the foot to heal properly. There are

also some other issues that can arise, such as nerve damage, foot deformities, etc. [1]. All these problems are extremely dangerous, even for healthy people. Legs, knees, and backs can also be affected because postures change to relieve the pain, which patients mostly do unconsciously [2].

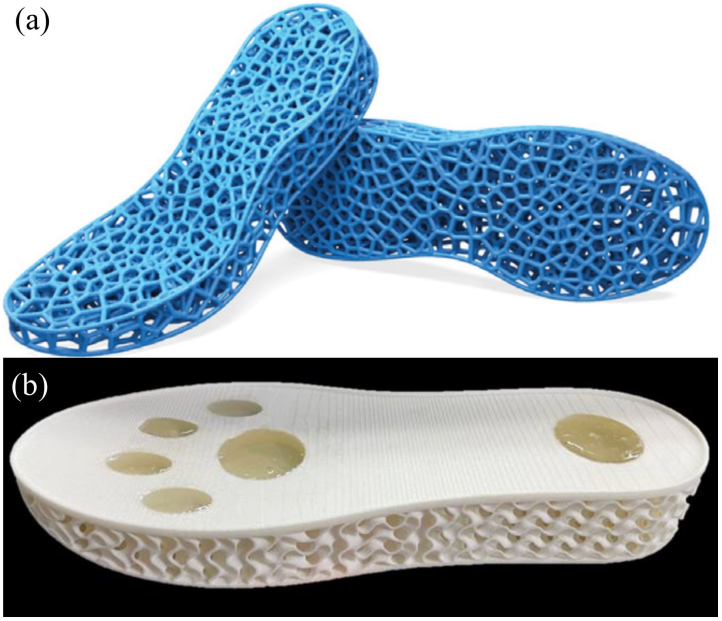

FIGURE 1.1: 3D printed midsoles: (a) Voronoi strut midsoles [3], (b) Gyroid lattice midsole [4] © adapted under CC BY-SA 4.0.

Along with stress, thermal comfort is another concerning matter. The thermal protection characteristics of footwear play an important role in confining heat inside footwear, particularly in hot environments. As the feet are dense with sweat glands, high temperatures inside the shoe induce sweating. High levels of foot discomfort from heat and perspiration can happen because of this.

Overall, having a pair of supportive, safe, and customized shoes that can adjust to the features of your feet is crucial. But traditional shoe-making processes struggle to meet the customization requirements of consumers due to the high costs of producing customized molds for different customers. Traditionally used materials in midsoles such as polyurethane (PU), ethylene-vinyl acetate (EVA), and polyethylene (PE) foam can alleviate in-shoe pressure, but they have poor breathability and heat transfer properties. These materials include porosity, which provides lightness and comfort,

but the porosity varies depending on the manufacturing method, and its distribution is extremely difficult to vary.

While many studies have been conducted on plantar stress reduction, there is a research gap in which several objectives, such as thermal comfort, manufacturability, and aesthetics, can be taken into account altogether. Unfortunately, seeking globally optimal solutions for multi-objective, non-convex problems can take exponential time with the number of variables, and formulating mathematical functions for non-quantitative objectives, i.e., aesthetics, is quite a challenging task. Further, there is a need for an effective search space from which different designs can be created in order to promote diversity and increase the chance of finding a global optima. All these give me the motivation to propose an effective method to generate diverse solutions for midsole design and search for the best ones as per various objectives.

1.2 Concept overview

We are accustomed to building load-bearing structures out of dense solids, but our nature contains numerous cellular structures [5, 6, 7]. They have a foamy or honeycomb-like core and a denser outer shell, increasing the shell's resistance to kinking or local buckling failure. Cork and wood are examples of natural materials with prismatic, honeycomb-like structures, whereas the inner cores of plants and bones are made of polyhedral cells. Some examples of natural cellular materials are shown in Fig. 1.2. Cellular structures can be classified as irregular or regular, having randomly scattered cells or an organized cell assembly, respectively [8]. Foams are an example of an irregular structure, while lattice structures are an example of a regular structure.

The number of struts and joints is a factor in the Maxwell stability criterion [9], which determines whether a structure shows stretching or bending-dominated behavior. Foams are bending-dominated structures, whereas lattice structures can be both bending-dominated and stretching-dominated [10]. Fig. 1.3 displays the stress-strain

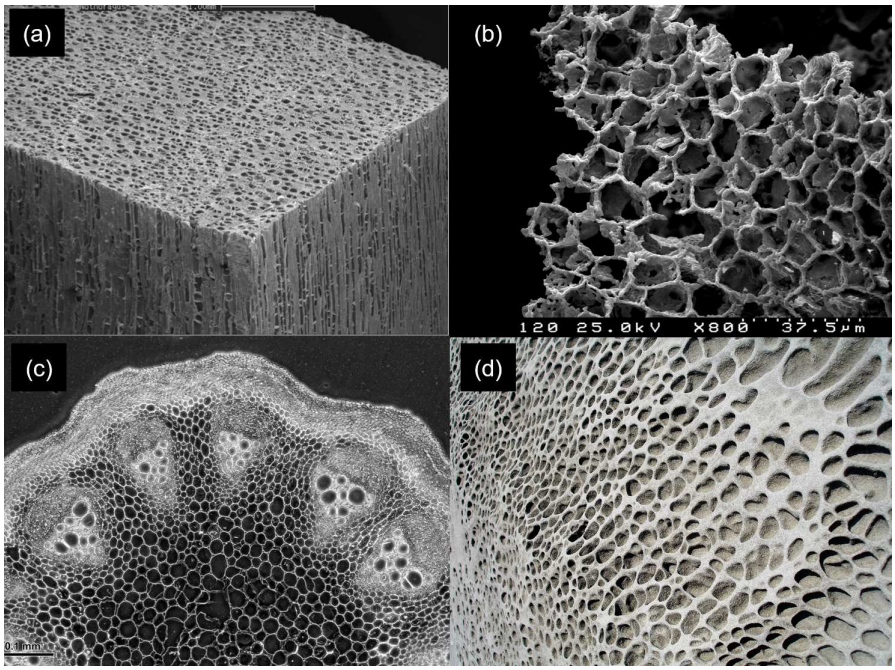

FIGURE 1.2: Examples of cellular materials in nature: (a) balsa wood (b) cork (c) inner core of a plant stem (d) trabecular bone.

characteristics of bending and stretching-dominated structures. Materials that are primarily used for bending initially behave linearly, then start to become plastic, and finally reach a stress plateau. Stretch-dominated materials first behave linearly, then the struts buckle, then there is post-yield softening and a stress plateau, and finally there is densification. Cellular materials' capacity to absorb energy and provide comfort is one of their key qualities in the form of foams [11]. Due to the low density of the cellular structure, which deforms elastically, foams are good energy absorbers. When bending-dominated materials, such as foams, are loaded under compression, they reach a stress plateau at some point. The goal is to reach a stress plateau below the foot's damaging threshold, where the foam should provide protection. This also prevents the foam from reaching densification levels under normal operating conditions. Because of this, the foam does not wear out, but some of the impact energy is nonetheless conveyed to the foot without damaging it.

There is a substantial difference in scale between foam and lattice structures. The development of lattice structures is preferable since the foaming process and tooling

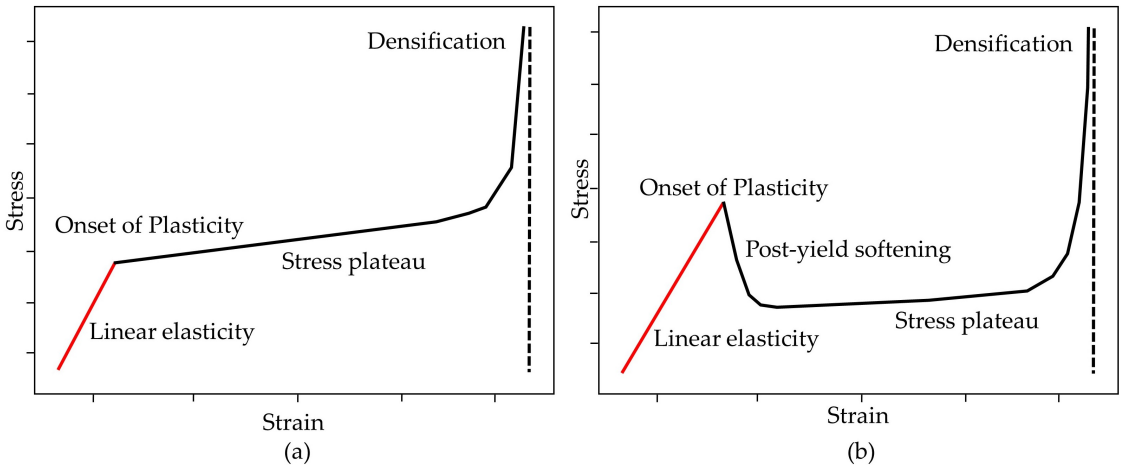

FIGURE 1.3: (a) Bending dominated behaviour of cellular structures, (b) Stretch dominated behaviour of cellular structures

constraints restrict the design of foams. Lattice structures have several properties, such as being ultra-lightweight, having a high stiffness-weight ratio, a low thermal expansion coefficient, and a high heat dissipation rate through active cooling [12]. However, as most lattice structures exhibit a stretch-dominated behavior, they are less suitable for purely energy absorption applications like foam because a long, flat plateau in the stress-strain curve would be needed. But when designing a midsole for a shoe, it's important to balance both strength and flexibility. The midsole needs to be strong enough to support the foot and resist compression while also being flexible enough to absorb shock and provide a comfortable ride. If the midsole lacks flexibility and is overly rigid, it may fail to offer adequate support, potentially causing discomfort or even harm. On the other hand, if the midsole is too soft and flexible, it may not provide enough support and could lead to instability or overpronation. Bending dominant structures can provide flexibility and comfort for midsole applications, but it may not be as strong as stretching dominant structures under compression. So to strike the right balance, stretching dominant structures can be used to give both strength and flexibility to a certain limit. In addition, as additive manufacturing works on a layer-by-layer approach, each strut is printed in several layers, and a bending-dominant structure might not be

perfectly suitable as bending occurs mostly because of shear force on a strut. So stretch-dominated lattice structures can be considered a meaningful way to regulate the performance of the midsole. The struts and joints used in the lattice structure of midsoles come in various topologies and sizes. They can be modified to change their physical and material characteristics, which will distribute ground reaction forces more evenly across the structure and reduce the force that impacts the foot. Beside stress relief, the midsole lattice structure will give more ventilation opportunities to the shoe sole, as in normal cases, it is the worst heat conductor of a shoe [13]. Though we can expect a very small amount of conduction heat transfer as elastomers have very low thermal conductivity, due to technological development, a highly thermally conductive elastomer is now available that we can use to manufacture the lattice structure [14].

Lattice structures may be categorized into three groups: periodic, conformal, and random [15]. The periodic and conformal lattice structures have a repeated pattern of an individual unit cell [16, 17]. However, the uniform nature of these lattice structures often works for simple conditions only. When it comes to complex situations and multiple objectives, applying uniform structures may cause initial geometry to change, geometric continuity to deteriorate, and an inability to adapt to diverse loading circumstances. The struts in a random lattice structure are randomly connected with each other in the design space. This sophisticated topology gives more opportunities to satisfy various objectives simultaneously.

Among different kinds of topology, I observed that tetrahedral structures are widely used for their superior strength [18, 19, 20]. They are stretching-dominant structures, and they can satisfy Maxwell's criteria of rigidity [21]. Tetrahedrons, as a 3D simplex, can constitute any complex volume, regardless of form or topology. They are flexible and easily controllable, which can be employed to construct various lattice structures. In addition, the aspect ratio and quality of tetrahedrons (see Fig. 1.4) can correspond to various properties, including isotropic and anisotropic behavior. The concepts of isotropic and anisotropic materials are useful in designing lattice midsoles, as they relate to the way that materials respond to forces from different directions. Materials that

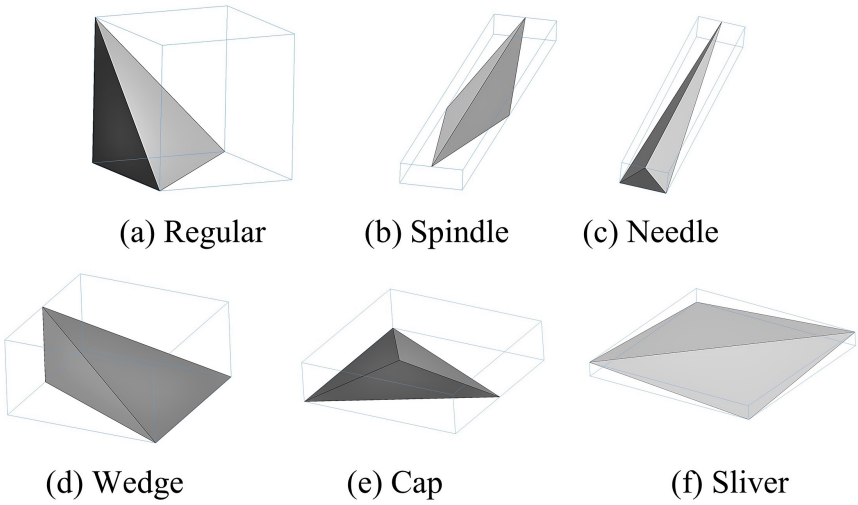

FIGURE 1.4: Tetrahedrons with various aspect ratios.

are isotropic share the same properties in all directions. This implies that regardless of the force's direction, they will react to it in the same way. Contrarily, anisotropic materials exhibit different properties in different directions. Accordingly, their reactions to forces will vary depending on the force's direction. Anisotropic behavior is expected from a midsole because the material properties and structure of the midsole are different in different directions. Midsoles are meant to have stronger stiffness and compression resistance in the vertical direction (i.e., perpendicular to the ground) to provide better support to the foot during impact with the ground. However, they are also engineered to be flexible in the horizontal direction (i.e., parallel to the ground) to allow for natural foot movement during walking and running. To satisfy these opposing demands, a midsole's anisotropic behavior is required. A midsole that is too flexible in the vertical direction may not offer enough support and shock absorption during impact, while a midsole that is too rigid in the horizontal direction can be uncomfortable and restrict the natural movement of the foot. Therefore, designers often use anisotropic materials and lattice structures to achieve the desired balance of stiffness and flexibility in different directions [22]. Many shoes, especially those made for running or other athletic activity, exhibit midsole anisotropy to achieve advanced functions [23]. Regular tetrahedrons (whose aspect ratio is 1) can be used to create structures that are desired to

have isotropic properties [24]. On the other hand, altering the aspect ratio can create a nonuniform, anisotropic, and lightweight structure for shoe midsoles. All these factors make tetrahedrons a good option for creating midsole structures, and I hypothesize that varying the shape and size of tetrahedrons within the midsole increases the diversity of midsole designs and thus finds better midsole structures for multiple objectives.

Although manufacturing diverse midsole lattice designs can be complex, it is feasible to create them using 3D printing technology. 3D printing has revolutionized the conventional shoe-making process, causing the footwear industry to evolve through software and computerized development technologies in terms of speed, efficiency, and customization. It can also fabricate cellular structures present in nature to create lightweight, high-performance products, and midsoles created using this technology are more appealing to customers nowadays. But each manufacturing technology has its constraints, and 3D printing is no exception. The quality of the lattice structure, such as surface quality, dimensional accuracy, residual stresses, support structure, etc., does influence the performance of the midsole lattice structure. Therefore, it is also crucial to consider all these factors together while optimizing the midsole's performance using a tetrahedral lattice structure.

1.3 Objective

The goal of this study is to develop a compact, fully automatic, multidisciplinary optimization method to improve the midsole's performance by utilizing tetrahedral lattice parameters. To compare the performance of the generated structures, the quantitative measurement for each of the objectives needs to be defined. For example, minimizing the peak stress of the midsole to reduce plantar pressure, maximizing the temperature difference to increase thermal comfort, defining a manufacturing index to measure manufacturability, and developing an aesthetic index based on surveys to consider user preferences. Moreover, a simple yet effective optimization algorithm is necessary to explore a wide range of midsole designs with increased diversity, which can help designers identify novel solutions that might not be discovered using traditional design

methods. The research question this study is trying to answer is: *How to obtain a midsole lattice structure that will give an overall good balance between different crucial objectives responsible for human comfort and aesthetic preferences?*

1.4 Scope

To test the hypothesis of using tetrahedral mesh for diverse designs, the tetrahedral mesh generation technique is applied here to the development of lattice structures for shoe midsoles. Also, by carefully selecting and updating the shape parameters using swarm intelligence, we can generate diverse tetrahedral structures within the design domain. Specifically, the design domain is a 3D volume bounded by the foot scan of a user and a flat plane. As such, this is a customized domain for the user, and the result will be total contact with the user's feet. The boundary of the design domain is then used as the input for tetrahedral mesh generation. The tetrahedral properties, such as radius-to-edge ratio, dihedral angle, and volume, are used as the generative parameters to generate tetrahedral meshes with distinct shapes and qualities. A thickening operation is performed on the mesh edges to form cylinders, and thus the connectivity of a tetrahedral mesh forms a lattice structure. The exploration and searching in the solution space are done by an enhanced version of Particle Swarm Optimization (PSO), which increases the diversity of the locally optimized results.

The contributions of this work are summarized as follows.

- A new framework to optimize custom midsole structure considering multidisciplinary objectives, like mechanical, thermal comfort, manufacturing, and aesthetics.
- Applying tetrahedral mesh generation to the construction of midsole lattice structures with distinct properties.
- Enhancing swarm intelligence for the exploration of midsole designs with increased diversity.

The thesis is organized as follows: Related works are reviewed in Chapter 2. A detailed discussion of this FEA model, tetrahedral parameter selection, and finalized optimization algorithm is given in Chapter 3. To further validate the proposed method, a case study of a midsole to compare different design configurations and further experimental verification is given in Chapter 4. And the work is concluded in Chapter 5.

2 Literature Review

2.1 Related Works

In this chapter, a thorough overview of the works related to lattice structure is provided, including their manufacturing and midsole performance enhancement. The previous works are categorized into different sections: cellular structure modeling and optimization, midsole performance improvement, footwear thermal performance, and additive manufacturing of lattice structures.

2.1.1 Cellular structure modeling and optimization

Cellular structure modeling is a crucial process for visualizing product designs, verifying modeling methodologies, and ensuring production quality. Computer-aided design (CAD) software is commonly used for the functional design and modeling of periodic and conformal cellular structures, but it offers limited control over parameters and design flexibility. Direct modeling software is typically used for porous structures with array characteristics, such as lattice and honeycomb. To address the limitations of commercial software, secondary development is also performed in some work to generate complex porous structures. For instance, SolidWorks is used by [25] to model irregular porous structures. Similarly, controllable Voronoi porous structures are designed by [26] by integrating Grasshopper into Rhino's graphic algorithm editor. However, these methods have limitations, such as fewer adjustable parameters, poor plug-in compatibility, and limited software permissions.

In recent years, various generative approaches have been developed to overcome the limitations of traditional CAD software and achieve automated design processes,

including those focused on cellular structure modeling as well as topology and shape optimization. A novel parameterization method is presented in [27] that seamlessly incorporates topology and shape optimization for the automated design of truss systems. This innovative approach not only resolves the issue of discontinuous surface geometry but also makes the acquisition of data necessary for shape optimization easier. The genetic algorithm and L-system are combined in [28] to optimize complex branched structures. The L-system design variables form the genome, generating a range of solutions for a multi-objective design problem. A new model for creating strut-based lattice structures is presented in [29]. Using a particle tracing algorithm, this model can automatically generate lattice structures based on user-defined and geometrical constraints for additive manufacturing. The concept of swarm intelligence is utilized in [30] to enhance the diversity of topology-optimized designs through a novel generative design method. By incorporating a rule of principal direction and applying it to form-finding using swarm intelligence, this approach also produces superior results compared to the original topology optimization method, particularly for more complex problems. A Non-uniform Cellular Automata algorithm is introduced in [31], that uses non-identical cells and a modified FSD/FUD approach to solve the minimum weight optimization problem for truss structures, considering both stress and displacement constraints. Shape grammar is combined with structural optimization processes in [32] to minimize the weight of grid shells and diagrid tall buildings with triangulated patterns. The structural feasibility is assessed with numerical analyses, and the optimized patterns are identified by means of the genetic algorithm.

The generative approaches discussed here offer new and innovative methods for designing cellular structures, and tetrahedral lattices are a promising class of structures that can benefit from these methods and be optimized for specific mechanical properties. Tetrahedral lattices are randomized lattice structures that have the capability of totally automatic construction in an arbitrarily shaped space. Research indicates that tetrahedral lattices offer a greater compressive strength-to-weight ratio [18] and impulsive response [33]. A numerical algorithm is developed in [20] to generate

conformal lightweight structures using a tetrahedral mesh. The authors discussed the effects of lattice design parameters on the relevant density change. Furthermore, they fabricated the designed cellular structures with a DLP printer and evaluated their mechanical properties by compression tests. Different combinations of various tetrahedral mesh parameters, i.e., cell size and density, strut diameter, and strut intersection rounding, can be used to determine the best balance of lattice parameters. Research has shown that strut diameter and strut intersection rounding are the best parameters to maintain strength and reduce weight [19]. The compressive mechanical behavior of 3D tetrahedral lattice materials is investigated in [34] by experimental and numerical methods, where the length-diameter ratio is considered a lattice parameter. The results indicated that the length-diameter ratio is inversely related to the relative density, strength, and energy absorption properties. However, most of the previous research related to tetrahedral lattice structures has focused on cell size. Strut diameter, strut intersection rounding,length-diameter ratio, or relative density are not intrinsic properties of tetrahedrons but are common in any kind of lattice structure. There are a number of other parameters related to tetrahedorns, like the radius-to-edge ratio, the minimum and maximum angle between the two faces of a tetrahedorn, etc. Using these parameters can provide more customization opportunities to improve the compressive load behavior of tetrahedral lattice structures. Although there are numerous studies on the optimization of lattice and truss structures from a multidisciplinary perspective, there are hardly any studies on tetrahedral lattice structures based on midsole application as well as utilizing the lattice parameters.

2.1.2 Midsole performance improvement

Numerous studies have been conducted to date to enhance midsole performance. Every shoe design has always taken into account a few key elements throughout the design

phase, such as weight, breathability, flexibility, shock absorption, strength-to-weight ratio, etc. Several studies are focusing on materials [35, 36, 37]. Most materials have porosity to provide lightness and comfort, and the porosity varies according to the manufacturing process. But these materials offer less design freedom and are thus very difficult to tailor to specific applications. A midsole design that considers body weight index also helps to improve an individual's footwear comfort. The effects of sole designs on plantar pressure are studied in [38] over a period of time in three different scenarios of walking, running, and jumping.

Designing the midsole's structure using lattice structures is another effective technique to control performance. With the rapid development of additive manufacturing technology, lattices have been used more frequently in midsole structural design because of their excellent properties. The directional energy performance of midsole structures is assessed by [23] which makes use of the lattice's anisotropic property. When the midsole structure increases energy in the desired direction, energy efficiency is enhanced. Four different topologies i.e Diamond, Grid, X-shape, and Vintiles have been considered in [39] to generate conformal lattice structures. Both numerical and experimental analysis have been performed in this work, and they found that the plantar stress is highly influenced by the lattice topology, where diamond performed the best among all lattice structures in terms of plantar stress reduction. For numerical analysis, the Finite Element Method is used in this work. For experimental analysis, the human foot heel was created using PLA and data from scans. It was installed on a test instrument and utilized as a sort of indenter for compression tests on the TPU lattice-filled sole midsoles. Not only the plantar pressure but also the vibration damping mechanism are affected by different topologies of the midsole. Alternating gradient lattice structures are studied in the shoe sole in [40]. With the increased difference in vibration level, this type of lattice structure has better cushioning performance than that of the uniform lattice structure. Along with lattice structure, total Contact Inserts (TCIs) tool is also used in literature to customize shoe soles that fully conform to the bottom surface of patients' feet. By focusing only on manually segmented high-pressure regions,

the Gaussian Progress Regression (GPR) model is utilized to figure out the relationship between lattice parameters and peak plantar pressure [41]. However, manual segmentation has some problems. Changing the lattice diameter at the contact point of two lattice struts can result in discontinuity as well as stress concentration at the joints. Previous studies prove that the mechanical properties of lattice cell structures are influenced by many factors, such as cell topology and geometry. But the geometrical parameters of lattice cell structures include cell size, strut angle, length, diameter, and aspect ratio, which are related together, and changing one parameter will definitely affect the others. However, the effects of the aforementioned parameters on a particulate lattice are not discussed in these works.

Uniform lattice structures may not be enough for more complex requirements, and thus some works use partitioning in their designs. Previous research indicates that dividing plantar regions based on anatomical characteristics and designing variable-dimension helical (VDH) springs based on local planter pressure looks promising for improving stiffness, energy absorption, and energy return of the midsole [42]. In other work, a multifunctional shoe midsole design method is proposed incorporating functionally gradient wave springs at the critical areas of foot pressure (heel, forefoot, and toe) and gradient cellular structure in non-critical areas [43]. The authors also studied the load-bearing capacity, energy absorption, stiffness, and cushioning properties of the midsole via compression testing. However, in partition design, the geometry and mechanical characteristics are not continuous at boundaries, and those locations where layers are connected and regions are in touch with one another are the weak sections of the structure, which are prone to breakage and damage during wear.

To generate lattice structures for the entire domain, a widely used approach is to use a voronoi diagram and convert its boundaries to lattice structures. In order to create variable-density midsoles, Grasshopper, a commercial software plug-in, is used to combine biomechanical data with the 3D Voronoi diagram [44]. A similar kind of work is proposed in [3], the authors Proposed a voronoi strut midsole structural design

method driven by plantar pressure distribution and Compared the mechanical performance with the centroid Voronoi strut midsole. However, using this kind of cell can be difficult to incorporate directly into an optimization algorithm, as creating a Voronoi diagram can be computationally expensive, especially when dealing with a large number of seed points or a complex spatial domain. Additionally, further post-processing is needed to ensure a smooth transition of struts at the design boundary. This complexity can make it difficult to optimize the seed points within a reasonable amount of time. Bio-inspired TPMS lattice midsole structures are also available in the literature [4] for attenuating ground impact, but there are several limitations that need to be considered while using TPMS lattice structures, especially for optimization, such as structural complexity and computational expense due to the high number of variables and constraints involved.

2.1.3 Footware thermal performance

Besides reducing plantar pressure and improving mechanical performance, thermal property is another factor in the comfort of footwear since foot temperatures can go beyond the comfortable range even for indoor gaits [45]. The properties of indoor sport shoes are constantly being improved, e.g., durability, grip, stability, comfort, etc. Recently, more attention has been given to the amount of heat a shoe can dissipate. A human foot acts as a thermal radiator for the body [46] and is dense in sweat glands [47]. During gait motion, a human's body weight cyclically compresses a shoe sole, generating heat during loading conditions. Footwear temperatures up to 50^{o}C have been measured in summer during exercise [48] and the human body must maintain its temperature at a value close to 37^{o}C [49]. During an average (90-minute) indoor training session in handball or volleyball, the shoes can become very warm and sweaty [13]. Cooling the foot may therefore affect the comfort of footwear. To serve this purpose, the focus should be on the midsole, as the sole of the shoe is the worst heat conductor. This has been validated by doing experimental research on the ventilation properties

of different shoes using a controlled heat source, a digital thermometer, and a thermographic camera [13]. How different zones participate in heat dissipation is presented in [49], where the temperature and the plantar pressure are measured during the running of an athlete at low and high speeds. The temperature in three different zones has been recorded from the lower face of the foot: the toes, the arch, and the heel. It should be noted from the observation that the temperatures remain practically constant throughout the standing time. Beside all the experimental studies, a thermal analysis model is also available in the literature to evaluate the thermal effects of shoe sole internal heat generation on foot comfort [50]. In the analysis, the heat is primarily transferred by conduction in a one-dimensional coordinate system.

There are also some studies focusing on the shoe material. Most prefer the mesh fabric sports shoes as their walking shoes because the leather sports shoes trap more heat and moisture on the feet [51, 52]. However, according to the evaluation of [53] in comparison to polyurethane, 3D printed thermoplastic polyurethane, and leather insoles, textile-fabricated insoles show no significant changes in foot skin temperature. However, a significant reduction in the relative humidity of the skin of the sole is found. All these previous works provide some inspiration to incorporate optimization of the thermal performance of the midsole. A combination of thermally conductive material with proper structural optimization that results in higher heat transfer through conduction and convection from the foot looks promising for bringing comfort to the human foot.

2.1.4 Additive manufacturing of Lattice structure

Lattice structures have a complex structure, so making them using traditional manufacturing techniques is not feasible. Additive manufacturing (AM) opens up new opportunities for the design and development of lattice structures [54, 55]. In recent years, AM has grown in popularity in the sports business, not just among professional players but also among the general public. It began in motorsports and cycling but has since developed into a crucial tool for producing running shoes, particularly midsoles. As a result, top sports equipment manufacturers like Adidas, Nike, and New Balance are

collaborating with technology companies that supply printer technology and appropriate materials, including Acrylonitrile Butadiene Styrene (ABS), Polycarbonate (PC), and Polylactic Acid (PLA) [56]. Rubber-like materials, such as TPU, are also appropriate for these applications due to their durability, elasticity, high tear and abrasion resistance, high resistance to dynamic loading, and good thermal resistance [57].The two main 3D printing technologies for producing shoes, and more specifically, shoe soles, are DLP and SLS. But till date, the most common one is the Fused Filament Fabrication (FFF) process [58], which has some limitations on printing lattice structure in terms of accuracy, and several studies have been done focusing on it. Different parameters have different influences on the fused filament fabrication (FFF) process on lattice structures, and the optimum level and significance of each process parameter vary with the orientation of the struts [59]. Material and printer type are also other factors that should be taken into consideration while printing miniature lattice structures. According to research [60], for PLA and ABS, the material as well as the 3D printer type have a significant impact on printability. Even though the surface quality and accuracy issues could not be fully resolved while printing lattice with PLA and ABS, they are capable of bearing compressive loads. However, the materials considered were rigid in the above cases, and as this kind of research is highly dependent on the material, the obtained information is not completely applicable to flexible materials, for example, TPU. Considering this direction, the mechanical behavior of lattice materials based on flexible thermoplastic polyurethane (TPU) is analyzed in [61] with honeycomb and gyroid architecture fabricated by 3D printing. The honeycomb lattice structure was found to provide rigidity, strength, plasticity, and energy absorption for the flexible TPU lattice compared to the gyroid. However, how the printing quality is affected is not discussed in this work. All these works indicate one thing: printing lattice structures, both flexible and rigid, using traditional FFF technology is quite challenging, so it's critical to consider the printing quality of lattice structures when optimizing them since it greatly depends on the strut thickness, overhang angle, and support material.

3 Methodology

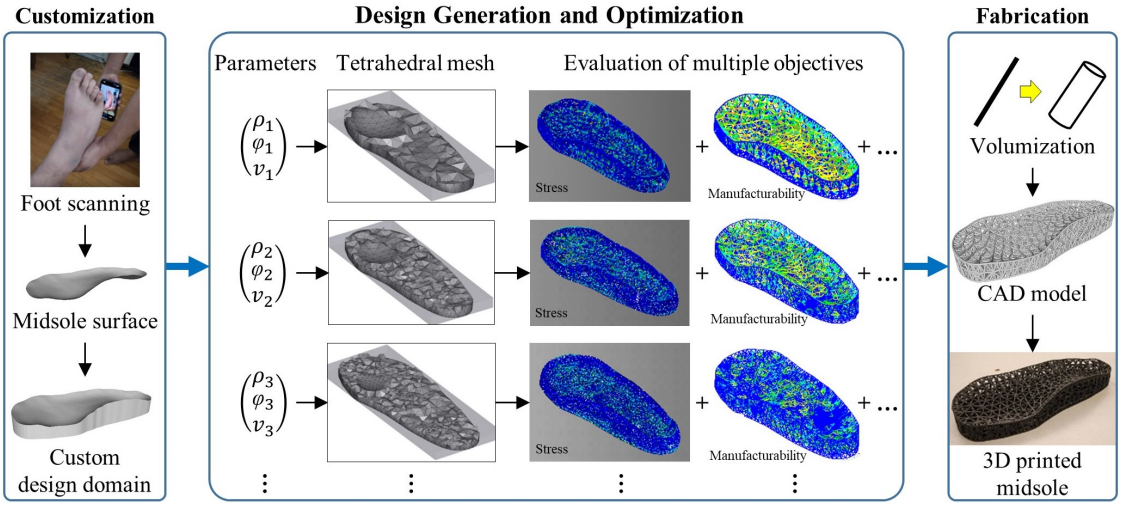

FIGURE 3.1: Overflow of the proposed method

Fig. 3.1 shows an overview of the present method. To achieve total contact in a custom shoe sole, the input is obtained by scanning the bottom surface of a foot. This defines the upper surface of the design domain for the midsole, which is then used to generate various lattice structures. The tetrahedral parameters have been used to create the tetrahedral mesh. The generation process employs a diversity-enhanced particle swarm optimization technique. Subsequently, the generated structures are evaluated based on a combined metric that considers multiple objectives. Technical details for each of these steps are provided in the following subsections.

3.1 Design Domain for Custom Midsole

To create a customized midsole design for each user, the Foot ID app [62] is used on an iPhone 13 to perform a detailed 3D scan of their foot. This app utilizes the TrueDepth

camera system, which includes sensors, cameras, and a dot projector, to capture both infrared images and dots. This data is then fed into neural networks, which generate a precise mathematical model of the foot. Next, only the bottom surface of the reconstructed foot is extracted and used as the input for the framework. The scan surface is aligned with the $x-y$ plane at a user-specified height, assuming the $x-y$ plane at $z=0$ is the ground. Although the bottom of the shoe can be of any shape, it is assumed to be flat for simplicity. The bottom surface of the design domain is obtained by projecting the scan surface onto the ground. The top and bottom surfaces were then joined with a strip at their boundaries to define a closed volume for the design domain. The first column of Fig. 3.1 shows the basic steps of creating a design domain for a custom midsole. This kind of shoe surface is designed to conform to patients' feet and increase the contact surface between the foot and shoe. This technique helps to accommodate deformities and relieve areas of excessive pressure by evenly distributing pressure over the entire plantar surface [63]. Even though the cost of making such a customized shoe insole is much higher than that of conventional shoe insoles, research results [64, 65, 66] have shown that this can be considered one of the most efficient ways to reduce peak plantar pressure. Finally, uniform remeshing is performed on the design domain to preserve sharp edges and prepare a proper triangular mesh for the next step.

3.2 Tetrahedral Mesh Generation

Lattice structures give more flexibility and feasibility to adjust the structural density as infillings. The tetrahedron holds the characteristics of randomness and continuity, and it is easy to change the structural topology by controlling tetrahedron design parameters. Randomness does not, however, ensure a good-quality mesh. To achieve high accuracy and efficiency in the simulations, a good-quality tetrahedral mesh is necessary. A tetrahedral mesh can be used to numerically simulate physical phenomena using numerical methods like the finite element and finite volume methods. Therefore, a Delaunay-based tetrahedron is used as the skeleton of the midsole's lattice structure design in this work.

A Delaunay triangulation for a given set of points in a general position is a triangulation such that no point in the set is inside the circumcircle of any triangle. A 3D Delaunay triangulation is called a Delaunay tetrahedralization. For every Delaunay tetrahedron, the circumsphere has to be empty, ensuring that the tetrahedra in the mesh do not contain any "skinny" elements and are well-shaped while maintaining proper connectivity. Fig. 3.2 shows Delaunay triangles and Delaunay tetrahedrons. Using this

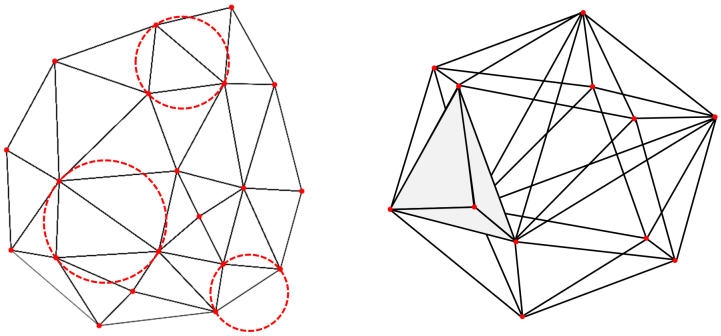

FIGURE 3.2: (a) Delaunay triangles, (b) Delaunay tetrahedrons

approach, domain boundaries (edges and faces) are respected and can be preserved in the resulting mesh with good mesh quality.

3.2.1 Generative Parameters for Lattice Generation

In tetrahedral mesh generation, different types of tetrahedrons are combined to create a mesh that accurately represents the geometry of the object being modeled while minimizing the number of tetrahedrons required. Regular tetrahedrons are often used in regions of the mesh where the geometry is relatively simple, while other tetrahedrons are used in regions where the geometry is more complex. Sliver tetrahedrons should be avoided as much as possible, but when they are necessary, they are combined with other tetrahedrons to improve the accuracy of the mesh. As the present method uses tetrahedral mesh generation to construct lattice structures and explores diverse solutions based on a set of input parameters, it is important to set up these parameters properly.

The process of generating tetrahedral meshes in this work is carried out using TetGen, an open-source program [67]. A variety of parameters are available in the program to govern the mesh generation process, such as input mesh preservation, maximum radius-to-edge ratio, minimum and maximum dihedral angles, maximum volume, mesh coarsening, mesh refinement, level of mesh optimization, number of added points, etc. While utilizing more parameters can yield a greater range of results, it also exponentially increases the computation time. Consequently, I have chosen to focus on the most important and influential parameters in order to generate tetrahedrons with distinct shapes and characteristics.

Maximum Radius to Edge ratio

The radius-to-edge ratio (ρ) of a tetrahedron (τ) is the ratio between the radius R of its circumscribed sphere and the length L of its shortest edge, i.e., $\rho(\tau) = R/L$, as depicted in Fig. 3.3a. For instance, a regular tetrahedron typically has a ratio of around 0.6, while a cap tetrahedron may possess a ratio larger than 2.0. Therefore, the radius-to-edge ratio represents a significant shape factor, and the maximum radius-to-edge ratio (ρ_{max}) is utilized as one of the controlling parameters. Regulating solely the maximum value of the ratio implies that certain tetrahedrons may have a lower ratio if it is the only way to meet other criteria. While an excessively low maximum ratio results in limited options

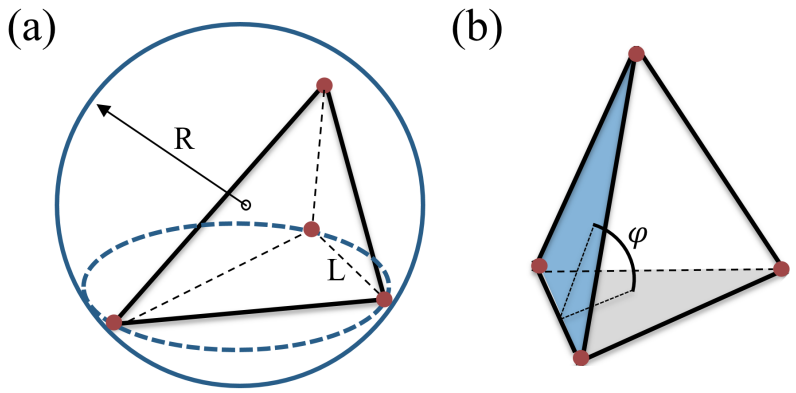

FIGURE 3.3: (a) The radius-to-edge ratio (R/L) and (b) the dihedral angle (φ) of a tetrahedron.

for available shapes to occupy the design domain and could lead to mesh generation failure, a very high ratio should also be avoided. Overly lenient constraints are, in essence, comparable to having no restrictions, resulting in identical outcomes.

Dihedral Angle

Second, the dihedral angle (φ) is the angle between two faces of a tetrahedron and varies between 0° and 180° as depicted in Fig. 3.3b. Just like the interior angles of a triangle are interdependent, the dihedral angles of a tetrahedron also influence one another. When some of them are very large, the remaining angles must be very small, such as in a silver tetrahedron. Regular tetrahedrons have dihedral angles ranging from 60° to 90°. Therefore, the dihedral angle is another shape factor that has a direct relationship with the tetrahedral shapes. Since the dihedral angles are interrelated, regulating either the minimum or maximum dihedral angle to achieve various shapes is needed. In this study, I chose to control the minimum dihedral angle (φ_{min}).

Maximum Volume constraint

Each tetrahedron takes up a specific volume within the design domain, and as the size of the tetrahedrons decreases, more of them are needed to fill the entire domain. This, in turn, has a direct impact on the number of struts in the lattice structure and its level of topological complexity. For the remaining parameters in the program, such as mesh refinement, mesh coarsening, etc., it is possible to use either the default values or choose values that do not conflict with other parameters.

3.2.2 Sensitivity Analysis of Generative Parameters

After identifying the key parameters in order to generate tetrahedrons with unique shapes and characteristics, a sensitivity analysis is performed to determine the range of the parameters. This analysis helps to limit the parameter values to effective ranges so that a distinct midsole lattice structure can be achieved while also reducing the computational time. The analysis is conducted by systematically varying one parameter at

a time while keeping the others at reasonable values and observing how the solutions change. This analysis has utilized the number of joints in the midsole lattice structure, which provides a clear indication of how the topology changes with parameter variation. However, it is important to note that this preliminary analysis is only intended to quickly narrow down the ranges and is not sufficient for eliminating all duplicate solutions. In this work, the solutions are generated using three tetrahedral parameters:

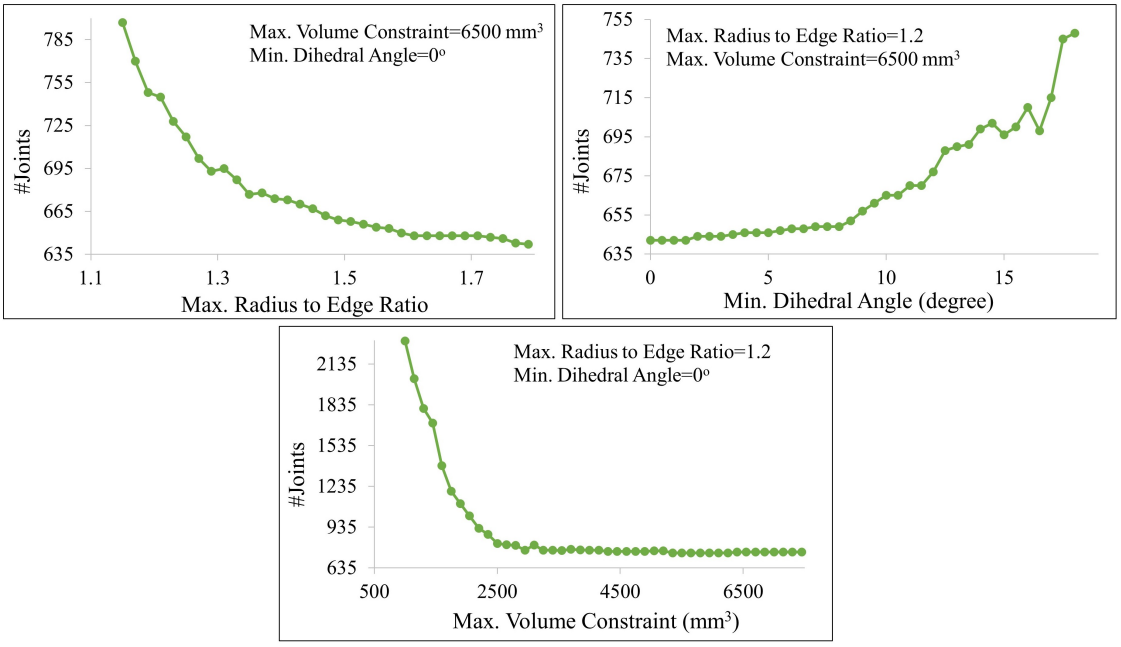

FIGURE 3.4: Sensitivity analysis for three tetrahedral parameters: the maximum radius-to-edge ratio, the minimum dihedral angle, and the maximum volume.

the maximum radius-to-edge ratio (ρ_{max}), the minimum dihedral angle (φ_{min}), and the maximum volume (V_{max}). The sensitivity analysis results are depicted in Fig. 3.4. For the maximum radius-to-edge ratio, any value below 1.15 fails to generate a mesh, while changes after 1.6 have minimal impact. Therefore, I used 1.15 as the lower bound and 1.6 as the upper bound, resulting in an effective range of [1.15 1.6] for this parameter. Regarding the minimum dihedral angle, the analysis shows that values above 18° result in a failure to generate a mesh, while values below this threshold work very well. Hence, the range of the minimum dihedral angle is [0° 18°]. Finally, the maximum volume parameter was found to have a lower bound of 1000 mm^3, as structures generated

with smaller volumes have too many thin struts that cannot be fabricated for the required midsole density. The graph clearly indicates a significant impact on the number of joints, which varies widely with changes in V_{max}. The plateau in the graph is reached around 6500 mm^3, but to provide a bit of extra room, the upper bound is set at 7000 mm^3. Thus, the range of the maximum volume is [1000 7000] mm^3. Based on the results of the sensitivity analysis, the table 3.1 summarizes the generative parameters and their range for obtaining diverse results. Additionally, all other parameters are listed.

TABLE 3.1: List of generative parameters and other parameters.

Parameters	Range/Value
Max. radius-to-edge ratio (ρ_{max})	1.15 to 1.6
Min. dihedral angle (φ_{min})	0° to 18°
Max. volume (V_{max})	1000 to 7000 mm^3
Max. dihedral angle	165°
Mesh Refinement	On
Mesh Coarsening	Off
Input Mesh Preservation	No

3.3 Parameter Exploration for Diversity and Optimization

After defining the design domain, generative parameters, and their respective ranges, the subsequent task is to identify an efficient approach for modifying these parameters. This is crucial for discovering the optimal structure while maintaining a diverse range of solutions. The five classical generative design techniques, namely genetic algorithms [68], swarm intelligence [69], cellular automata [31], shape grammars [70], and L-systems [71], employ rule-based methods to create new generations of designs by determining the new state of each parameter based on its current state as well as its neighbors. These techniques are typically used to search for solutions in an n-dimensional space, where n represents the number of design parameters. In this work, n = 3, as three parameters are considered. Not all generative techniques work for every domain, as different domains have different requirements, constraints, and objectives that may require different approaches and techniques. Generative techniques like cellular automata, shape grammars, and L-systems can generate a large variety of designs but

may require a significant amount of time to develop models, grammars, and rules, respectively. The Genetic Algorithm (GA) follows a set of heuristic rules inspired by the processes of natural selection and genetics, such as crossover and mutation operators, to explore the search space. On the other hand, Particle Swarm Optimization (PSO), which is a type of swarm intelligence, is inspired by the social behavior of birds flocking or fish schooling. Both of them have the ability to solve complex problems and handle multiple objectives efficiently. But PSO is renowned for its high speed convergence rate for both single and multi-objective optimization and maintaining diversity [72]. PSO generally converges faster than GA as it updates the particle velocities and positions based on exploration and exploitation [73]. In contrast, GA involves crossover and mutation operations, which can be computationally expensive and slow down the convergence speed. PSO has a simpler implementation compared to GA, as it involves fewer parameters to tune and requires fewer computational resources. This makes it easier to use and more suitable for problems with a smaller search space. As these two metaheuristic techniques do not guarantee finding the optimal solution but rather aim to find a good solution within a reasonable time frame, I focused on using PSO to get diversity and the final optimized design.

3.3.1 Diversity-Enhanced Particle Swarm Optimization

This work focuses on the development of a multidisciplinary optimization framework that couples Particle Swarm Optimization (PSO) with the parameters of a tetrahedral mesh. The fundamental principle behind the particle swarm optimization (PSO) algorithm involves the movement of a group of particles within a search space, where each particle represents a potential solution. The particles' movements are influenced by both their individual best-known position within the search space and the overall best-known position of the entire swarm.

The calculation of their velocity can be expressed as follows.

$$\mathbf{V_i} = w\mathbf{V_i} + c_1 r_1(\mathbf{P_i} - \mathbf{X_i}) + c_2 r_2(\mathbf{S} - \mathbf{X_i}), \tag{3.1}$$

where V_i is the velocity of particle i, w is the inertia coefficient (e.g., 1), $\mathbf{P_i}$ and $\mathbf{S}$ are the particle's and the swarm's best-known positions, $\mathbf{X_i}$ is the particle's current position, c_1 and c_2 are the local and global acceleration coefficients (e.g., 2), and r_1 and r_2 are randomly generated numbers in the range $[0, 1]$. Then, the particle's position is updated by the velocity.

$$\mathbf{X_i} = \mathbf{X_i} + \mathbf{V_i} \tag{3.2}$$

This process is repeated iteratively in order to explore potential solutions and ultimately discover a satisfactory solution. The PSO algorithm can be conceptualized as having three components guiding the particles' movement: an inertia component, a cognitive component, and a social component. The inertia component is the tendency to move in the same direction. The cognitive component reflects each particle's individual memory of its best-known solution ($\mathbf{P_i}$), encouraging exploitation by directing the particle towards its own best solution in the search space. The social component reflects the swarm's collective memory of the best-known solution ($\mathbf{S}$), encouraging exploration by directing the particle towards the best solution found by the entire swarm. As the particles move towards the overall best solution, they tend to converge towards a single solution, which allows them to escape from local optima and continue to search for better solutions. It is assumed that better solutions are located in the direction of the swarm's best position. However, if the initial positions of the particles are far from the global optimum, it may be challenging to discover them.

The argument here is that when the neighboring particles of the swarm's best position are functioning adequately, other particles should not move towards this position. Rather, they should prioritize enhancing diversity and exploring various local optima to maximize the probability of discovering the global optimum.

Hence, it is expected that the particles will exhibit the following behaviors:

Local search: They must find the best solution for the region where they are located.

Migration: Once they complete searching a local region, they should explore other local optima.

Division: They should prevent redundant efforts by avoiding searching the same region.

To achieve these behaviors, the following modifications are implemented to the algorithm:

Firstly, consideration of the swarm's best position (**S**) is removed, and a neighborhood factor is added to the social component. The velocity equation (Eq. 3.1) then becomes:

$$\mathbf{V_i} = w\mathbf{V_i} + c_1 r_1(\mathbf{P_i} - \mathbf{X_i}) + c_2 r_2(\mathbf{N_i} - \mathbf{X_i}), \tag{3.3}$$

where $\mathbf{N_i}$ denotes a neighboring position of $\mathbf{X_i}$, and c_2 is now a neighboring coefficient.

Secondly, a particle is forced to focus on searching its local region by eliminating the social component's influence. This is done by setting c_2 to 0, which causes the particle to move solely according to the cognitive component, thereby looping around its best position due to inertia.

Thirdly, when a particle is unable to discover better solutions after five local searches, a negative coefficient is assigned to the cognitive component ($c_1 = -2$) to move the particle out of the local region and explore other areas. This process stops when the particle finds a better solution, after which it switches back to the local search. Finally, during migration, if a particle is in close proximity (2% of the search space size) to an explored region, it steers itself away from that direction by setting c_2 to -2 and $\mathbf{N_i}$ to the closest explored position. To summarize, the coefficients are established based on the expected behaviors as follows:

$$w, c_1, c_2 = \begin{cases} 1, 2, 0 & \text{for local search} \\ 1, -2, 0 & \text{for migration} \\ 1, 0, -2 & \text{for division.} \end{cases} \tag{3.4}$$

The flowchart of the diversity-enhanced PSO algorithm is depicted in Fig. 3.5. By reacting to the above-mentioned modifications, the particles not only search around the local best position but also move to other spaces for a better solution, and overall, a

combined behavior of group work is achievable to find a satisfactory solution until the termination criteria is satisfied (S is not updated for the last 15 iterations). Here, all the objectives are combined into a single cost function, giving weight to each of the objective cost functions. The process of combining them is elaborated on in the subsequent sections.

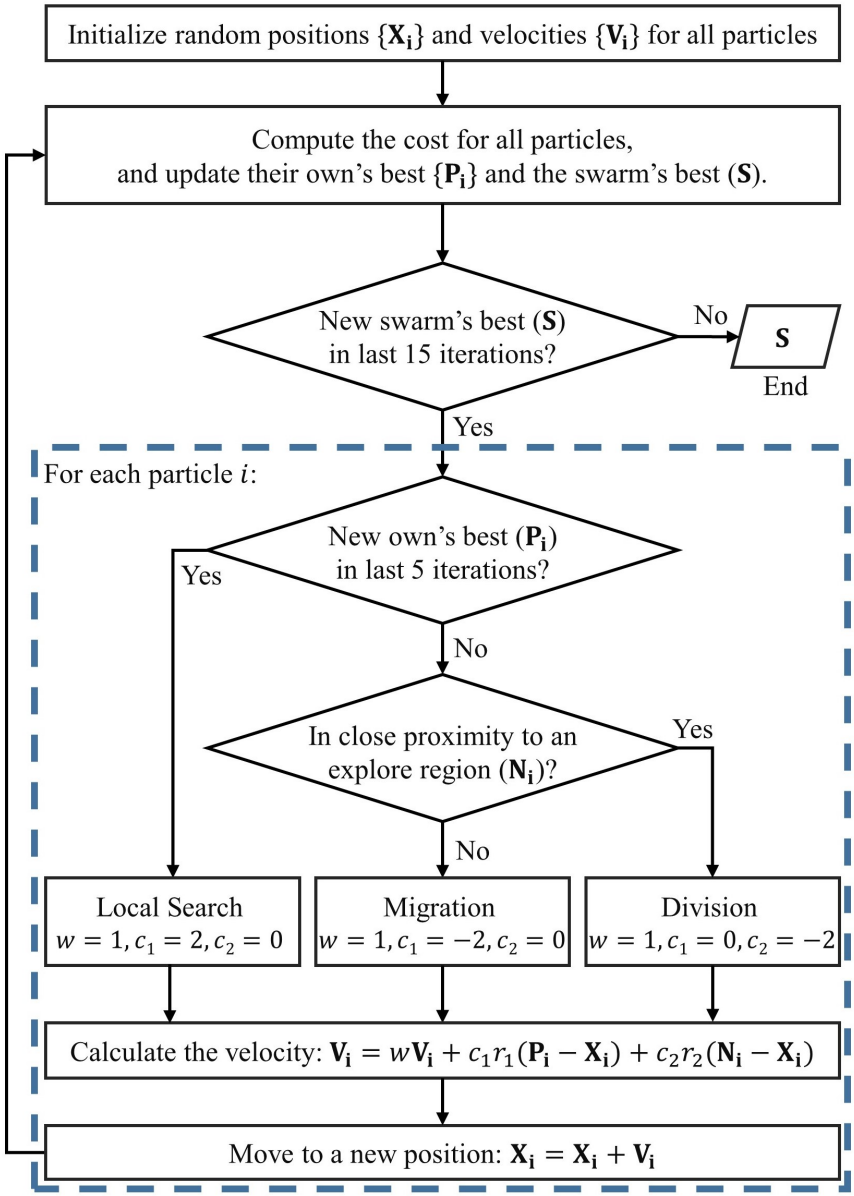

FIGURE 3.5: The flowchart of the multidisciplinary optimization framework.

3.4 Quantitative Measurement of Objectives

The generative approach is discussed in the previous section. However, to optimize the designs, a quantitative method of measurement is needed to determine which designs are better. This section aims to develop a measurement for each objective. Total four objectives are considered in this work: plantar stress (O_S), heat dissipation (O_H), manufacturability (O_M), and aesthetics (O_A). The optimization's cost function is the weighted sum of all objectives, i.e.,

$$Cost = w_1 O_S + w_2 O_H + w_3 O_M + w_4 O_A \tag{3.5}$$

The user can set the weights of the objectives according to their preferences, or they can use the default equally weighted values, where $w_1 = w_2 = w_3 = w_4 = 0.25$.

Combining multiple objectives into a single cost function has several benefits. A single cost function is easier to work with and optimize than multiple separate objective functions. It simplifies the decision-making process and reduces the complexity of the problem. Combining objectives into a single cost function allows for trade-offs between different objectives. In the cost function, the weight assigned to each objective reflects its relative importance compared to the other objectives. By allowing the user to set the weights of the four objectives in the optimization problem, the tool provides flexibility in addressing different needs. Each objective represents a physical aspect of the footwear design. Stress and heat dissipation are related to the structural and thermal behavior of the footwear, respectively, and are important for ensuring the safety and comfort of the user. The manufacturability objective considers the ease and efficiency of the manufacturing process, which can have an impact on the cost and time required to produce the footwear. The aesthetic objective is related to the visual appearance and style of the footwear, which is an important factor in the consumer's purchasing decision. If a designer prioritizes manufacturability and aesthetics over stress and heat dissipation, they can increase the weight of those objectives accordingly. On the other

hand, if the designer is more concerned about the structural integrity and thermal performance of the footwear, they can put more emphasis on stress and heat dissipation objectives, respectively.

The framework is designed to optimize computational efficiency by allowing users to exclude any objectives that are not deemed necessary by assigning a weight of zero. It is recommended that the weights of the objectives add up to one, ensuring that the sum of the remaining objectives still adds up to one even if one of the objectives is excluded. All objectives are normalized during the creation of the objective function to avoid the impact of varying units and scales for each objective, resulting in a unit-less function that can be combined into a single cost function. For example, stress is measured in megapascal (MPa) while temperature is measured in (°C), so normalization is necessary to avoid the dominance of one objective over the others.

The main challenge in optimizing the designs is how to quantify the objectives, where the target is to minimize the cost using Eq 3.5. The following subsections provide a detailed description of each objective.

3.4.1 Plantar Stress Redistribution

Discomfort and health issues, especially for diabetic patients, can be caused by high plantar stress. Therefore, a midsole should be designed to reduce these high pressures and provide accommodative support. Since the user's weight cannot be changed, most studies focus on redistributing the plantar stresses to achieve uniform stress distribution throughout the foot. This means reducing the peak stress as much as possible and bringing it closer to the average stress. Although direct measurement of peak normal stress at the bottom surface of the foot is a common approach to achieve this objective, this work chooses to minimize the maximum stress of the midsole for the following reasons:

Firstly, the forces applied by the foot on the midsole and the forces exerted by the midsole on the foot are a pair of action and reaction forces. When the stresses in the midsole are evenly distributed, these forces are also uniformly distributed.

Secondly, reducing the maximum stress on the midsole structure for the same applied loads indicates that the structure is more robust and can withstand higher loads without failure.

Thirdly, it is worth mentioning that many foams and plastics exhibit hyperelastic behavior, whereby stress increases exponentially after the strain surpasses a certain threshold. By reducing the maximum stress, the midsole can undergo greater deformation and maintain full contact with the foot, thus avoiding stress concentration. Finite Element

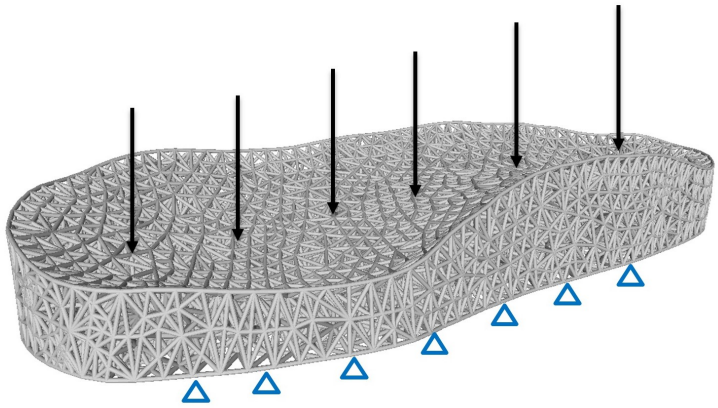

FIGURE 3.6: Applied conditions for mechanical analysis

Analysis (FEA) is performed in this work to numerically investigate the mechanical response of the lattice shoe sole under compression load. To obtain information about the maximum stress (S_{max}), MatLab is used to script the Ansys Parametric Design Language (APDL) to run the Ansys Mechanical solver. The material property is considered an isotopic property. It is noteworthy to highlight that these kinds of lattice structures are mainly manufactured using 3D printing technology. Layer-by-layer deposition in Fused Filament Fabrication (FFF) creates microstructures that are different from those created by traditional manufacturing methods, and the mechanical properties of printed parts are significantly affected by FFF process parameters such as build and raster orientations, layer height, filament width, and infill patterns and densities [74, 75, 76]. However, these effects are not considered in FEA to keep the analysis simple. In FEA,

it is common practice to assume a homogeneous material with isotropic properties, excluding the impacts of the FFF process parameters. Incorporating these effects into the FEA would introduce additional complexities, requiring more intricate modeling and extensive experimental data for accurate representation. By simplifying the analysis, it is possible to capture the structure's fundamental behavior without extensive parameter calibration. In the simulation model, each strut of the lattice structure is represented by a one-dimensional (1D) beam element. This idealization significantly reduces computation time by providing a simpler simulation method. The loading and boundary conditions are shown in Fig. 3.6. The bottom surface, assumed to be in contact with the ground, has a fixed boundary condition, while a downward load, simulating a foot stepping on it, is applied to the top surface. Previous research [77] indicated that the reaction force in jumping can reach about three times one's weight (see Fig. 3.7).

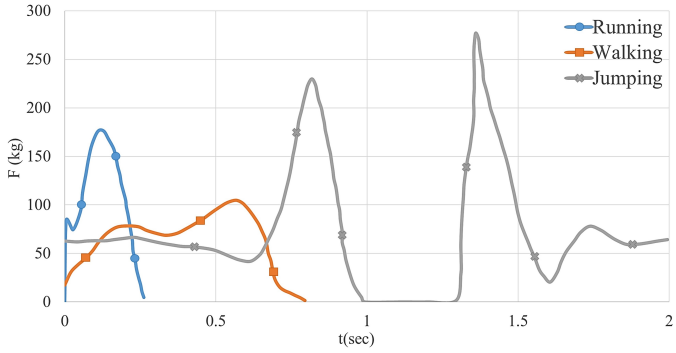

FIGURE 3.7: Reaction force in different scenarios for a healthy man of 84.6 kg[77]

Therefore, the load is 240 kg, evenly distributed across the entire top surface, considering the human weight of 80 kg. For a single midsole, the final load is considered to be 120 kg, assuming the load will be equally distributed across the entire top surface. Since the maximum stress (S_{max}) could have a unit of megapascal, which is a large value of 10^6, adding it directly to the cost function may significantly affect the optimization. To avoid biasing the optimization towards the maximum stress objective, normalizing the scale is needed among all objectives. So here, the tensile strength (TS) of the material is considered as a reference, and a safety factor of 0.5 is used to obtain a normalization factor. The maximum stress is then divided by this normalization factor to obtain the

normalized objective function, which is expressed as:

$$O_S = \frac{S_{max}}{0.5TS}.$$

3.4.2 Heat Dissipation

According to Kinoshita and Bates [48], a foot wearing a shoe can become as hot as 50°C during exercise, making it crucial for a shoe to dissipate heat effectively to prevent discomfort.

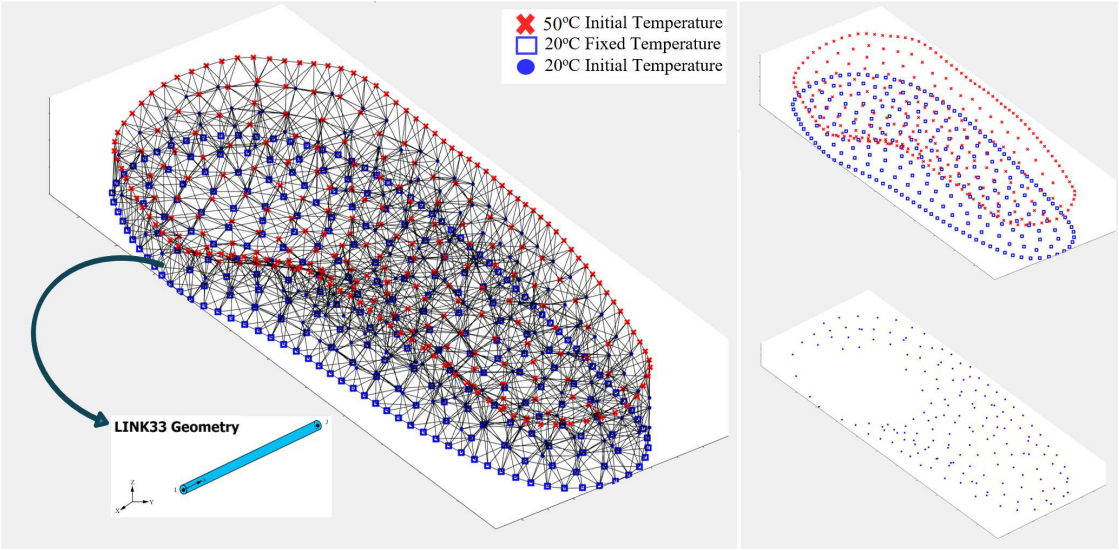

FIGURE 3.8: Applied conditions for thermal analysis.

To assess a shoe's heat dissipation ability, thermal analysis is performed with the boundary conditions depicted in Fig. 3.8. The top surface's initial temperature is set to 50°C to simulate the foot's temperature because research has shown that the temperatures remain practically constant throughout different zones at standing time [49]. The bottom surface's temperature remains fixed at 20°C, assuming it is in contact with the ground. All other nodes' initial temperatures are 20°C. Similar to the mechanical analysis, the transient thermal analysis employs Ansys APDL, and each strut uses the LINK33 element, which is a uni-axial element with the ability to conduct heat between

its nodes. The 1D transient heat conduction equation is defined as:

$$\frac{\partial}{\partial x}\left(k\frac{\partial T}{\partial x}\right) = \rho c_p \frac{\partial T}{\partial t} \tag{3.6}$$

Here, x represents the direction of heat transfer of each strut, T is time in sec, ρ is the density of the material in kg/m^3, K is the thermal conductivity in W/m^oC, and c_p is the specific heat capacity in J/Kg^oC. To simplify the analysis, only thermal conduction is considered here since free convection heat transfer has a negligible effect. As the top surface's temperature decreases over time, the midsole structure removes heat from the foot more efficiently, improving foot comfort. Therefore, the aim here is to minimize the highest temperature (T_{max}) on the upper surface after a fixed time duration, which I set to 10 seconds in this work. To balance the scaling effect among different objectives, the temperature value is normalized by using the given highest temperature and the skin temperature. (37°C) [49]. The objective function is defined as:

$$O_H = \frac{T_{max} - 37}{50 - 37}.$$

3.4.3 Manufacturability

Additive manufacturing (AM) opens up new opportunities for the design and development of cellular structures. AM has good control over the shape and size of struts, the topology of the structure, and many other features. However, dimensional accuracy and surface quality are some factors of the lattice structure that should be considered while printing them. Ensuring manufacturability is crucial in achieving a successful design, as any manufacturing defects (as shown in Fig. 3.9) can impede the product's intended functionality. In the case of 3D printing the shoe midsole using fused filament fabrication (FFF), it is important to consider the limitations of this method [59, 60, 61]. Strut length and overhang angle are critical factors that affect print success, and a manufacturing index is defined here to quantify the manufacturability of a lattice structure based on its geometry. Short struts can be printed at any angle due to bridging, and struts with an overhang angle less than a certain angle can be printed regardless

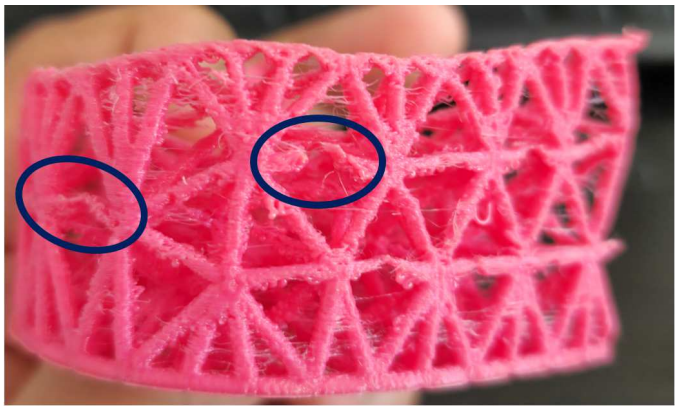

FIGURE 3.9: Manufacturing defects by FFF 3D printing.

of their length, as they are self-supporting. For longer struts, print quality depends on both length and overhang angle, requiring consideration of both factors to determine manufacturability. A score can be assigned to a lattice structure to provide a measure of its manufacturability, taking all these factors into account. However, these geometric factors are not universal, and they are also dependent on the printing material, printer, and process parameters. Assuming that the same material, printer, and settings will be used, a trial print can be conducted with struts of varying lengths and overhang angles to update the thresholds for calculating the manufacturing index.

For instance, by employing an Ultimaker 3 with a print height of 0.1 mm, a print speed of 12 mm/s, a print temperature of 225°C, and 100% infill, I established the strut length threshold to be 5 mm and the overhang angle threshold to be 45°. Next, a manufacturing score (M) is assigned, between 0 and 1, to each strut (s) based on its length (L) and overhang angle (θ) using the following approach:

$$M(s) = \begin{cases} 1, & \text{if } L < 5 \text{ or } \theta < 45^\circ \\ \frac{1}{2}\left(\frac{5}{L} + \frac{90^\circ - \theta}{45^\circ}\right), & \text{otherwise} \end{cases}$$

The first scenario has a score of 1, indicating that the print is always successful. The second scenario consists of two components. The first component is a measure of how much longer the strut is than the length threshold, resulting in a lower value for longer struts. The second component is a measure of how much larger the overhang angle

is than the angle threshold, with a maximum angle of 90°. A lower value is assigned to larger angles. Both components have a range of 0 to 1, and a factor of $\frac{1}{2}$ is multiplied to generate a score ranging from 0 to 1. The manufacturing index of a structure is computed by taking the average score of all its struts and subtracting it from one, as a higher score implies better performance. However, the manufacturing index does not start at zero since even the worst strut has some good struts nearby. For example, in a typical joint with six struts, two of them might have a score of 0 due to their length and horizontal orientation, but the other four should still have high scores. To address the scaling effect, the manufacturing index is normalized further by dividing it by 0.34:

$$O_M = \frac{1}{0.34}\left(1 - \frac{1}{|s|}\sum_s M(s)\right)$$

Midsole Print Orientation

As the Manufacturing Index (O_M) is mainly focused on strut length and orientation information, it is applicable to any midsole orientation. The print orientation will change the layer orientation, which will affect the strength, stiffness, and other mechanical properties of a 3D-printed part in a number of ways. For instance, a part printed with the layers aligned perpendicular to the applied load will typically be weaker and less rigid than one printed with the layers oriented in the direction of the applied load. In normal cases, the midsole structures are inclined at such an angle that several midsoles can be printed on a single print bed, and changing the orientation can also improve the manufacturing quality. The proposed framework also keeps that in mind. The user needs to give the orientation information before calculating the Manufacturing Index (O_M) and it will be calculated based on the orientation information. Fig. 3.10 shows a midsole inclined at different orientations and their correspondent Manufacturing Index. In the case of Fig. 3.10b, tilting the midsole at a different angle increased the Manufacturing Index. But further tilting can also decrease it from the previous case (see Fig. 3.10c). However, finding out the optimal angle for the best manufacturing index in tilted conditions is beyond the scope of this research.

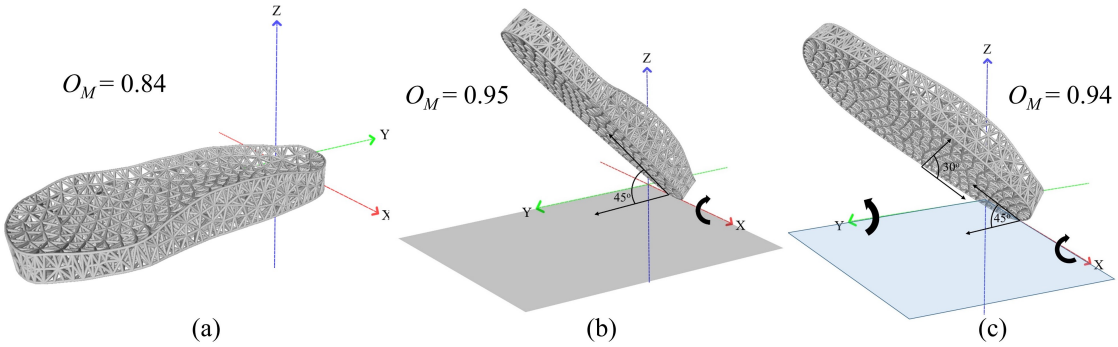

FIGURE 3.10: (a) Midsole in normal direction, (b) Midsole rotated 45° (counter-clockwise) with X-axis, (c) Midsole rotated 45° (counter-clockwise) with X-axis and 30° with Y-axis respectively.

3.4.4 Aesthetics

Design aesthetics play a critical role in influencing consumer purchasing decisions. However, quantifying and measuring them remains a challenging task, as different people can have different preferences. In this regard, I conducted a survey to investigate some visual design factors for tetrahedral midsoles. However, it is important to note that the goal of this work is not to develop a comprehensive method for aesthetic measurement. In the survey, 54 participants were asked to rank several midsole structures

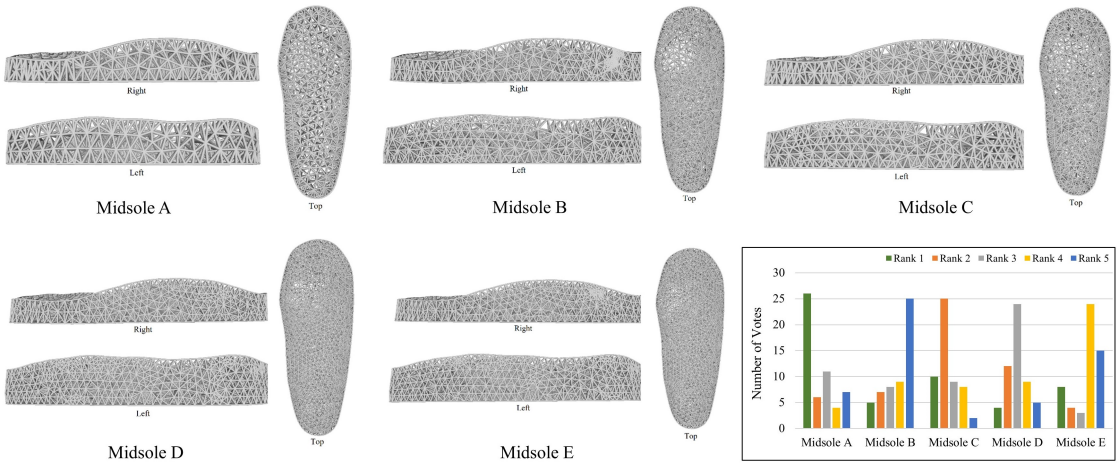

FIGURE 3.11: Different midsole structures considered in the survey and the ranking result.

on a scale of 1 to 5 based on their aesthetic preferences by providing the top, left, and right side views of the midsoles. Participants rated how much they liked the midsoles as a potential customer. The midsole they liked the most was ranked as 1, and the least

favorite was ranked as 5. At the time of designing the survey, the important factors were unclear. Therefore, five tetrahedral midsoles were selected based on the difference in mesh size. The midsoles and their corresponding rank distribution are depicted in

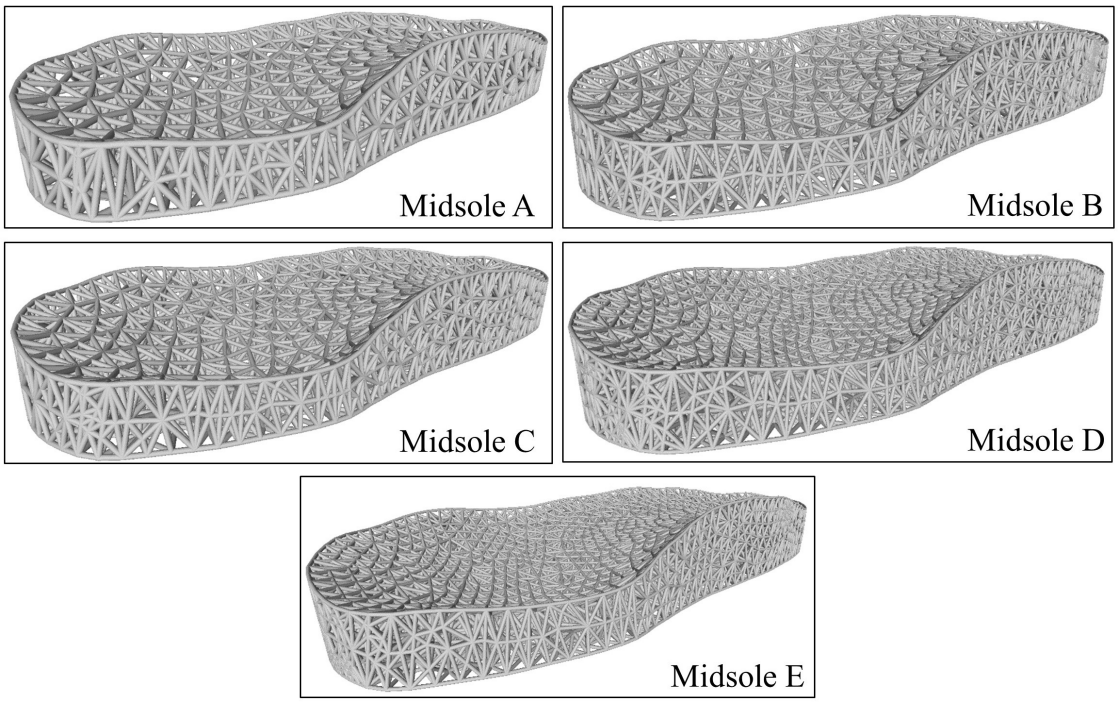

FIGURE 3.12: Isotropic view of different midsole structures considered in the survey.

Fig. 3.11 and the isotropic views of the midsoles are given in Fig. 3.12. Although the survey results indicate that people have diverse preferences, one particular rank stands out for each midsole. Specifically, midsole A is ranked first, followed by midsole C, midsole D, midsole E, and finally midsole B. Upon further discussions with some of the participants, I discovered that they commonly considered two factors: structure density and uniformity. Participants tended to favor a coarse structure over a dense one, and they found that midsoles with more uniformity were more visually appealing.

For better comparability, the structure statistics are presented here for the midsoles in Table 3.2 according to their respective rankings. The number of joints is used in this work to provide an indication of structure density, as a higher number of joints implies a denser structure. Also, the percentage of strut lengths within one standard deviation (std) from the mean is employed here to denote the uniformity of the structure.

TABLE 3.2: Structure statistics of the midsoles in the survey, including the number of joints (#Joint) and the mean, the standard deviation (Std), and the percentage within 1 std from the mean (Std_1) of the strut length.

Midsole	Rank	#Joint	Strut Length		
			Mean	Std	Std_1
A	1	648	12.11	4.50	72%
C	2	1190	9.23	2.69	64%
D	3	3153	6.14	2.14	67%
E	4	3593	5.80	2.10	68%
B	5	2369	6.27	3.21	61%

The standard deviation is the measure of the spread of a set of data from its mean. The bigger the dispersion or variability, the higher the standard deviation and the greater the magnitude of the value's divergence from the mean [78]. A more uniform structure should have a higher percentage within the one std range (Std_1) indicating more struts near the mean. As shown in the table, the ranking is strongly correlated with the number of joints, with the exception of midsole B. Despite having fewer joints (2369) than midsoles D (3153) and E (3593), midsole B has the lowest uniformity (61%) and is ranked last. Midsole A has the lowest number of joints (648) and the highest level of uniformity (72%), making it the top-ranking midsole. To measure aesthetics for tetrahedral midsole structures, the data of #Joint and Std_1 is used here, as they showed good alignment with the survey ranking. To normalize the Std_1 part, I used the value of one minus Std_1 and divided it by 0.32, as 68% data are under Std_1 for a normally distributed data set. This will normalize the value to more or less than one compared to the Std_1 of normally distributed data. To normalize the #Joint, the reference considered here is the input mesh size (**I**), i.e., the foot scan. As the tetrahedral mesh must have a larger size than the input surface mesh, the input mesh size is multiplied by 5 to obtain the normalization factor. The objective function is defined as the average of the two values:

$$O_A = 0.5 \left(\frac{\#Joint}{5|\mathbf{I}|} + \frac{1 - Std_1}{0.32} \right)$$

4 Results & Discussions

The proposed method was implemented using Matlab on a PC with an Intel Core i5 6500 3.2 GHz processor and 16 GB memory. A solid-to-void ratio of 0.3 was established for the design domain, meaning that for denser structures, the struts were made thinner to ensure that all designs contained the same quantity of material. The material considered in this study is Ice9 Flex, produced by TCPoly (Atlanta, GA, USA), and its relevant material properties are listed in Table 4.1. However, this material utilized throughout the project has been exhausted and is presently unavailable from local vendors. Regrettably, at the time of writing this thesis report, I was unable to procure more. Despite having to use alternative materials to construct the designs that were originally intended for this material, the validation has not been compromised. These materials are thermoplastic polyurethane (TPU), produced by Ninjatek (Lititz, PA, USA), and polylactic acid (PLA), produced by Filaments.ca (Mississauga, ON, Canada). Their properties are also included in Table 4.1.

TABLE 4.1: Material properties of Ice9 Flex, TPU, and PLA used in this work.

Property	**Ice9**	**TPU**	**PLA**
Density (kg/m^3)	1400	1100	1240
Therm conduct (W/m-K)	8	0.15	0.13
Specific heat (J/kg-K)	1300	1210	1700
Elastic modulus (MPa)	95	12	2400
Tensile strength (MPa)	15	26	48
Shore hardness	88A	85A	70D

The optimization process involved randomly distributing 100 particles within the search space, with each particle initialized with a random velocity. The cost function for a given structure was computed in under a minute, and optimization converged after 41 iterations, during which the global best remained unchanged for 15 iterations

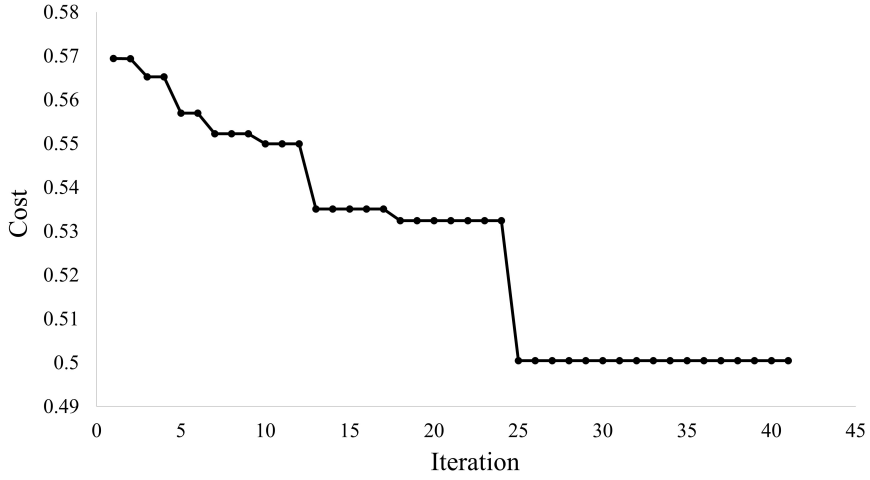

FIGURE 4.1: Convergence curve of the PSO optimization.

(see Fig. 4.1). The convergence curve shows several small drops, indicating effective local search, and large drops, indicating the discovery of new optima. Fig. 4.2 shows the particles' trajectories over the iterations, revealing that each particle focused on a specific region of the search space to maximize the chances of finding more optima. The twisted parts of the trajectory correspond to local optimization, while the extended parts indicate the particles' attempts to locate better local bests outside their current vicinity.

4.0.1 Validation of Generative Method

In this work, a generative approach is proposed to achieve a wide variety of designs and thus increase the chances of finding the global optimal solution. To verify the efficacy of this method, the best and worst designs are examined here for each objective among all the generated outcomes (refer to Fig. 4.3). This validation aims to assess whether the approach can truly generate diverse designs concerning the objectives.

To begin with, there is a significant difference between the maximum stress values of the best and worst structures for the planter stress objective (O_S). Specifically, the best structure has a maximum stress of 3.08 MPa, whereas the worst one has a much higher maximum stress of 7.46 MPa – more than twice as high as that of the optimal structure. In terms of heat dissipation (O_H), the most effective structure reduces the temperature at the top surface by 10.6°C, from 50°C to 39.4°C. In contrast, the least effective structure

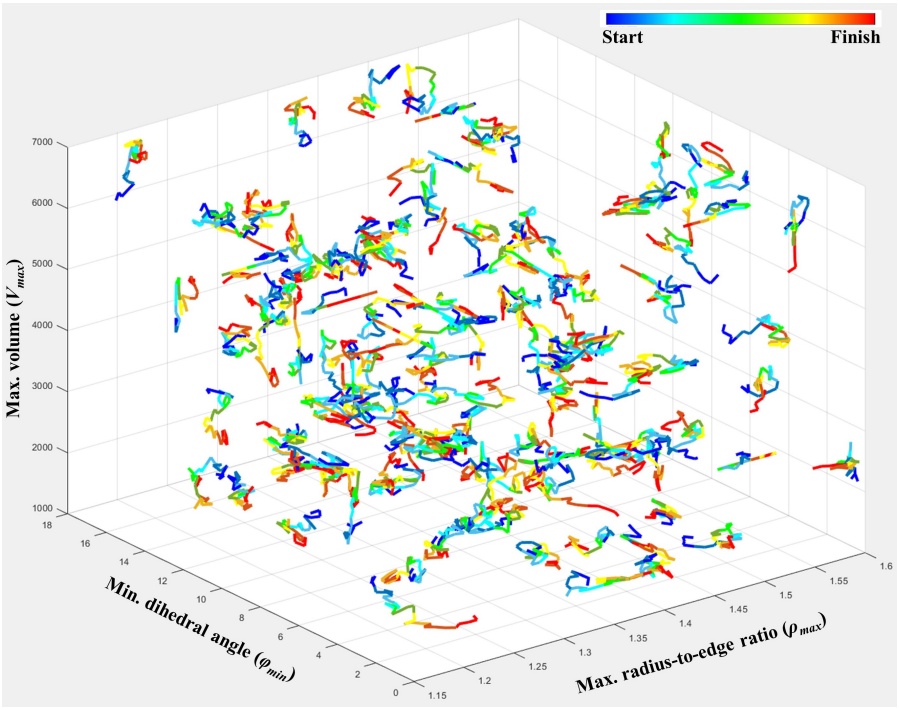

FIGURE 4.2: Trajectory of particles in the search space.

only lowers the temperature by 2.5°C, resulting in a top surface temperature of 47.5°C. In other words, the optimal structure is four times more efficient at dissipating heat than the worst-performing structure. Furthermore, the third column of Fig. 4.3 displays a color map that represents the manufacturing scores of the struts, with blue indicating good scores and red indicating poor scores. It should be noted that the manufacturing index (O_M) has an inverse relationship with the manufacturing score ($M(s)$). The best structure has a manufacturing index of 0.25, while the worst structure has a significantly higher index of 0.87 – a difference of 3.5 times between the two. Lastly, the aesthetics objective function (O_A) considers both the density and uniformity of a structure, with a lower value indicating higher aesthetic appeal. The optimal structure according to this function has a small number of joints (697) and a Std_1 value of 74.95%, resulting in an O_A score of 0.50. On the other hand, the least appealing structure has almost five times as many joints (3,873), looks dense, has a Std_1 value of 63%, and contains some non-uniform regions that are highlighted with zoom-in views. Its aesthetics index is 1.22, which is around 2.5 times higher than that of the best structure.

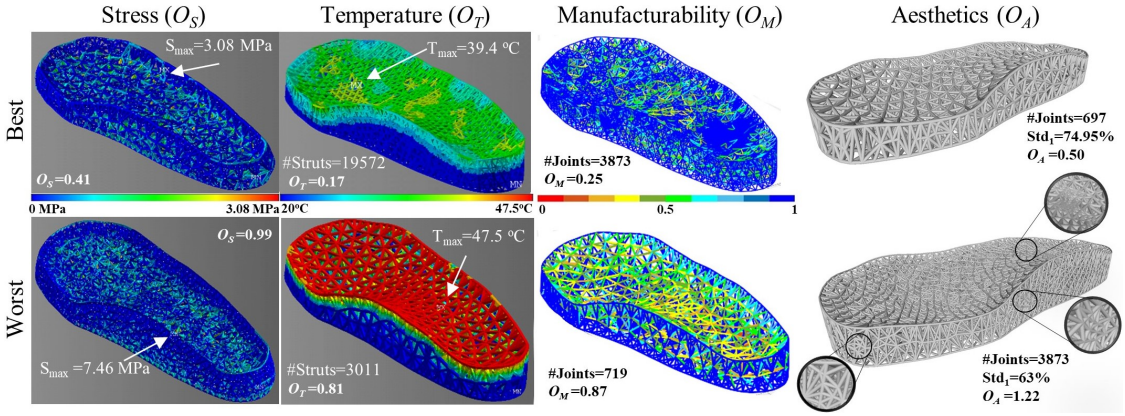

FIGURE 4.3: The best and the worst structures for each of the objectives separately.

To summarize, despite the optimization being targeted at the combined metric of all objectives, the generated solutions demonstrate varying levels of performance from the perspective of each individual objective. This confirms the success of the generative method, which uses tetrahedral mesh generation and diversity-enhanced swarm intelligence, in generating a range of diverse designs. Furthermore, the best structures for each objective are vastly different, with the best structure for heat dissipation being a densely packed one and the best aesthetics-focused structure being a more coarse one. Therefore, a trade-off must be made via a multi-objective optimization process.

The structure that performs the best overall for the combined metric is illustrated in Fig. 4.4. It demonstrates superior performance for most objectives, with $O_S = 0.45$ (the best O_S being 0.41), $O_T = 0.28$ (the best O_T being 0.17), $O_M = 0.39$ (the best O_M being 0.25), and $O_A = 0.86$ (the best O_A being 0.48). The differences between the maximum stress (S_{max}) and maximum temperature (T_{max}) of this structure and the corresponding best structures are only 10% and 3%, respectively. The aesthetics performance is the most compromised objective in this structure, mostly because a denser mesh is required to enhance other performances. Overall, this structure maintains a satisfactory balance between all objectives, proving the effectiveness of the proposed optimization approach.

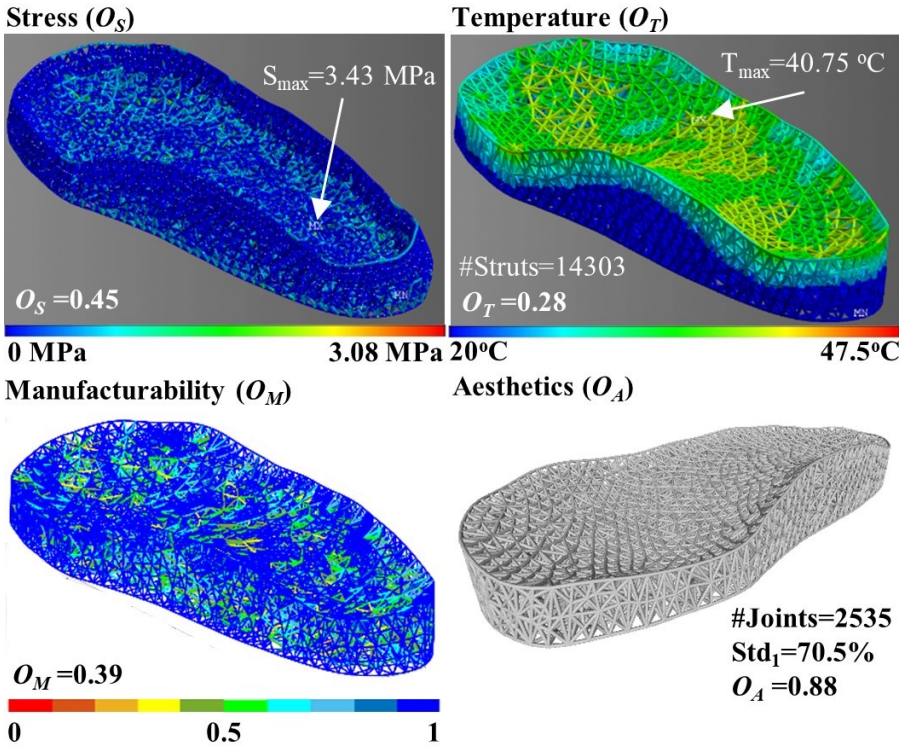

FIGURE 4.4: The overall best structure of combined objectives.

4.0.2 Thermal Validation

I fabricated the best and worst structures of thermal performance (second column of Fig. 4.3) to validate the quantitative measurement of heat dissipation. These midsoles were subjected to a thermal experiment. However, due to the unavailability of the Ice9 material, the midsoles were printed using the PLA material. The thermal conductivity of PLA (0.13 w/mK) is much lower than that of Ice9 (8 w/mK). However, improvements in a low-thermal-conductive material can lead to even greater improvements in a higher-thermal-conductive material. The fabricated midsoles with the experimental setup are shown in Fig. 4.5, with midsole 1 being the best and midsole 2 being the worst. Both midsoles were weighed to ensure that they had the same amount of material. To prevent thermal convection from causing heat loss, the midsoles were wrapped in insulators made of plastic wrap and aluminum foil. The bottom of the midsoles was in contact with cool water at 10°C, while the volume on top of the midsoles was filled with hot water at 50°C. The volume was approximately 750 ml, similar to the

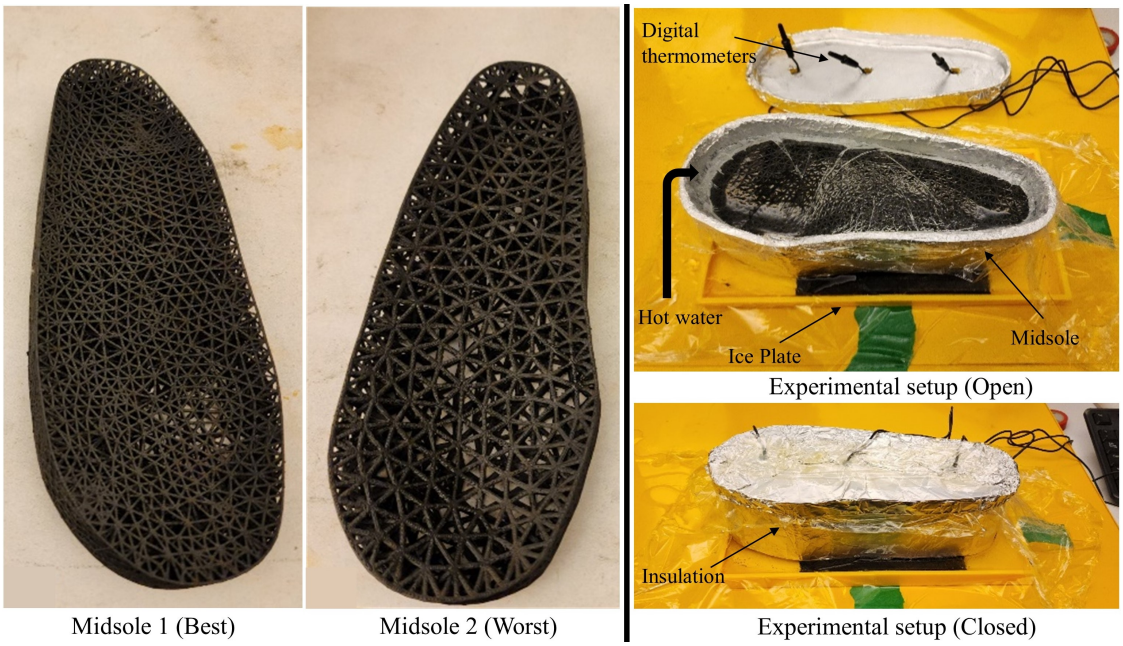

FIGURE 4.5: Midsole-1 (Best) and Midsole-2 (Worst) in terms thermal performance with their experimental setup.

volume occupied by a foot. To prevent the water from leaking, a thin plastic film was placed between the water and the midsole. The temperature was recorded at the heel zone, metatarsal zone, and toe zone every minute for 30 minutes using three Amropi aquarium thermometers to get a detailed temperature distribution in the midsole. Additionally, a FLIR ONE Pro thermal camera was used, manufactured by Teledyne Flir (Wilsonville, OR, USA), to capture temperature changes from the outside.

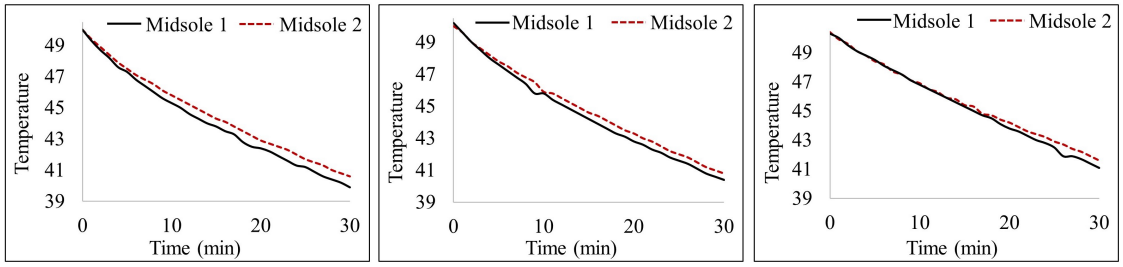

FIGURE 4.6: Inside midsole water temperature with time at Toe, Metatarsal, Heel area.

The thermometer data is presented in curves in Fig. 4.6. The plots reveal that the water temperatures decrease over time, but the rate of temperature change is greater in midsole 1 than midsole 2. After 30 minutes, the temperature differences between

midsole 1 and midsole 2 in the toe, metatarsal, and heel zones are 0.7°C, 0.4°C, and 0.5°C, respectively. Although the differences are not significant due to the low thermal conductivity of the PLA material, human skin is highly sensitive to temperature changes and can detect differences as low as 0.03°C [79]. Therefore, midsole 1 can dissipate more heat from the top surface than midsole 2, with the same amount of material.

Fig. 4.7 shows the thermal images. The images were taken at 0 min, 10 min, 20 min, and 30 min. The thermal images are consistent with the sensor data. Additionally, three points were chosen at the water-midsole interface for comparison, and they remained fixed throughout the experiment. At the start (0 min), the outside temperatures

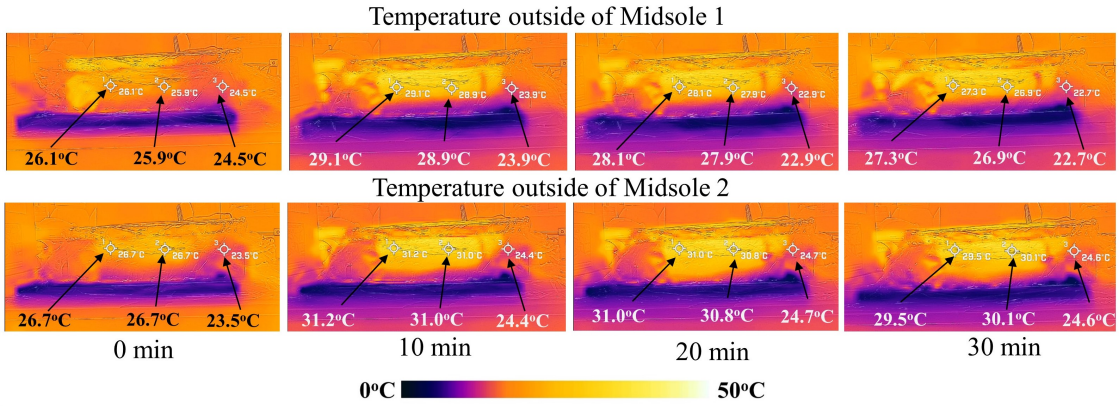

FIGURE 4.7: Thermal images of the temperature distribution outside the midsoles at different time intervals.

were close to room temperature and increased as the hot water was added. Thereafter, they decreased in sync with the water temperatures. For example, the leftmost point in midsole 1 had a temperature of 29.3°C at 10 min, 28.1°C at 20 min, and 27.3°C at 30 min. Conversely, the same point in midsole 2 had higher temperatures of 31.2°C at 10 min, 31.0°C at 20 min, and 29.5°C at 30 min. It can be observed from the photographs that for midsole 1, the outside temperature was consistently lower than for midsole 2. As the method of isolation was the same, for the same period of time, midsole 1 conducted more heat than midsole 2. Overall, the results of this experiment confirm that the quantitative measurement of heat dissipation is accurate and effective.

4.0.3 Comparison with Other Lattices

Other lattice shoe soles have been described in the literature [39, 3]. In order to compare the tetrahedral lattice structure generated by the proposed method with other structures, compression tests were conducted to determine their mechanical responses. The best performing structure in plantar stress redistribution (the best O_S in Fig. 4.3) was chosen, and other lattices, including grid, body-centered cubic (BCC), diamond, and Voronoi structures, were chosen and are shown in Fig. 4.8 with the experimental setup.

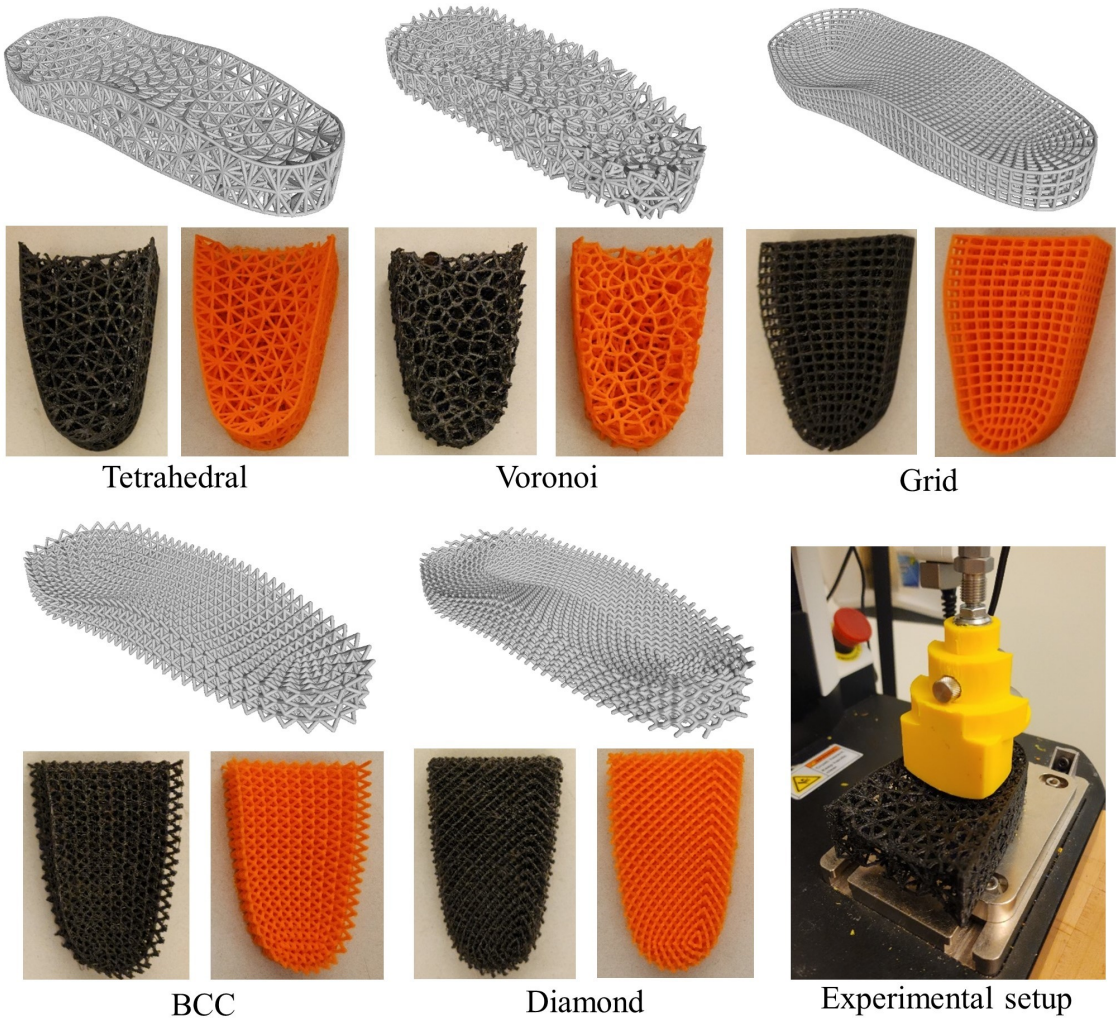

FIGURE 4.8: Different midsoles such as Tetrahedral, Voronoi, Grid, BCC and Diamond printed in TPU 85a(Black) and PLA(Orange) for the compression test.

The grid and BCC structures are relatively simple and regular, serving as a baseline for comparison. Diamond is known to be strong and has a tetrahedral-like structure,

with each joint having four neighboring joints. It can be viewed as a specific case of my results, as it is a uniform tetrahedral lattice. The Voronoi lattice is random and highly structurally complex, similar to the tetrahedral lattice. In fact, a Delaunay tetrahedralization is the dual of a Voronoi diagram. However, the connectivity and properties of the Voronoi structure are completely different due to its basic element being a polyhedron.

To ensure a fair comparison, all midsoles were designed with the same weight and strut diameter but differed in connectivity and number of struts. They were tested with both PLA and TPU to assess their performance in rigid and soft materials, respectively. The elasticity moduli of PLA and TPU are 2400 MPa and 12 MPa, respectively. Additionally, PLA has a more linear material property, while TPU is more non-linear. Only the heel portion of the foot was taken into account because it first absorbs the majority of the load. Since the testing was limited to the heel zone, only half of the midsoles were printed, and their weights were carefully measured to ensure equal amounts of material were used. A press-head was designed based on the surface of the heel zone and fabricated in PLA, which is strong enough to impart a compression force on the midsoles. The midsole samples were placed on a compression plate, and the press head was used to apply a uniaxial compression load. The Mark-10 ESM750SLC universal testing machine was used for the experiment, with a strain rate of 10 mm/min.

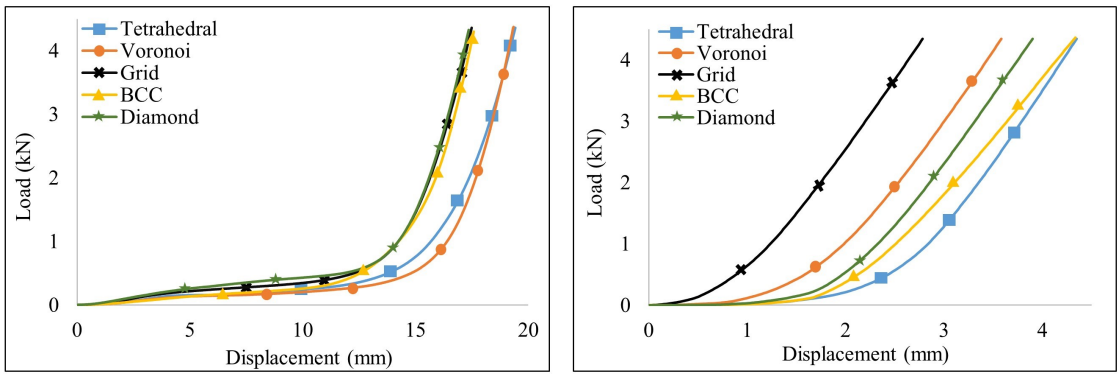

Load-displacement curves for TPU 85A

Load-displacement curves for PLA

FIGURE 4.9: Load-displacement curves for the TPU 85A and Load-displacement curves for the PLA.

The load-displacement curves were used to plot the testing results, which are visible in Fig. 4.9. In the case of TPU, the curves show little difference initially due to the softness of the material, but they diverge into two groups when the deformation is large. The first group, consisting of the grid, BCC, and diamond structures, exhibits a rapid increase in load at a smaller displacement than the second group, which includes the tetrahedral and Voronoi structures. This increase is due to the densification of the lattices, and the tetrahedral and Voronoi structures allow more deformation before densification, resulting in better contact with the foot and less stress concentration.

Looking at the load-displacement curves for PLA, the structures' differences are more apparent, with stiffness in the following order: grid, Voronoi, diamond, BCC, and tetrahedral structures. The load measured by the load cell above the press head can be viewed as the reaction force applied to the foot by the midsole. When this force is higher at the same displacement, it results in higher foot plantar pressure. The tetrahedral lattice structure exhibits greater compliance with the foot and better redistribution of plantar stress, making it an excellent choice for use in shoe midsoles.

5 Conclusion

A new approach for designing custom shoe midsoles using tetrahedral mesh generation and diversity-enhanced swarm intelligence is presented in this work. The method simultaneously optimizes four independent objectives: plantar stress redistribution, heat dissipation, manufacturability, and aesthetics, using a swarm optimization algorithm to vary the tetrahedral parameters and obtain diverse lattice structures. The diversity of these structures is validated, and the method is shown to not only achieve better results for a specific objective but also strike a balance between them to achieve an overall optimal structure. Experimental tests demonstrate that the tetrahedral structure generated by the proposed method outperforms other lattice structures.

Although the present method has shown promise, there are some limitations that need to be addressed. Firstly, the input mesh of the design domain remains fixed during optimization. While the tetrahedral mesh generation can make some changes to the surface mesh, they are not significant. To overcome this, future work involves adaptively refining the mesh based on high and low stress areas, with the aim of further reducing stress. Secondly, the stress analysis only applied a uniform load to the top surface of the midsole, which may not accurately represent real-world usage. Future work will apply plantar pressure distribution-driven approaches [3] to improve effectiveness. Thirdly, the stress analysis only considered linear material properties, whereas flexible materials exhibit non-linear behavior. To address this, a surrogate model will be developed to capture non-linear properties without compromising computational speed. Fourthly, the Finite Element Analysis (FEA) only considered the isotropic material property, which

is not the real case for structures printed using the FFF technique. Experimental methods [80] or computational models such as Classical Laminate Theory (CLT)-based approaches [81] or numerical homogenization techniques [76], can be utilized to predict the effect of printing process parameters on the elastic response of 3D printed parts with cellular lattice structures. Lastly, while this work developed quantitative measurements for four objectives, there are many other objectives for shoe midsoles, such as vibration and energy transfer. Future work will expand to include these objectives.

Bibliography

[1] Tatiana Almeida Bacarin, Isabel CN Sacco, and Ewald M Hennig. "Plantar pressure distribution patterns during gait in diabetic neuropathy patients with a history of foot ulcers". In: *Clinics* 64.2 (2009), pp. 113–120.

[2] Ricardo L Actis et al. "Multi-plug insole design to reduce peak plantar pressure on the diabetic foot during walking". In: *Med. Biol. Eng. Comput.* 46.4 (2008), pp. 363–371.

[3] Huaqin Cheng et al. "Design of three-dimensional Voronoi strut midsoles driven by plantar pressure distribution". In: *Journal of Computational Design and Engineering* 9.4 (2022), pp. 1410–1429.

[4] Yilin Xiao et al. "A 3D-Printed Sole Design Bioinspired by Cat Paw Pad and Triply Periodic Minimal Surface for Improving Paratrooper Landing Protection". In: *Polymers* 14.16 (2022), p. 3270.

[5] Lorna J Gibson, MF Ashby, and Kenneth E Easterling. "Structure and mechanics of the iris leaf". In: *Journal of Materials Science* 23.9 (1988), pp. 3041–3048.

[6] Michael F Ashby et al. *Metal foams: a design guide*. Elsevier, 2000.

[7] Trevor G Aguirre et al. "Bioinspired material architectures from bighorn sheep horncore velar bone for impact loading applications". In: *Scientific Reports* 10.1 (2020), pp. 1–14.

[8] Tochukwu George. "Carbon fiber composite cellular structures". PhD thesis. Ph. D. Thesis, University of Virginia, 2014.

[9] M.F. Ashby and Y.J.M. Bréchet. "Designing hybrid materials". In: *Acta Materialia* 51.19 (2003). The Golden Jubilee Issue. Selected topics in Materials Science and Engineering: Past, Present and Future, pp. 5801–5821. ISSN: 1359-6454. DOI: https://doi.org/10.1016/S1359-6454(03)00441-5. URL: https://www.sciencedirect.com/science/article/pii/S1359645403004415.

[10] Michael F. Ashby. "Cellular Solids – Scaling of Properties". In: *Cellular Ceramics*. John Wiley Sons, Ltd, 2005. Chap. 1.1, pp. 1–17. ISBN: 9783527606696. DOI: https://doi.org/10.1002/3527606696.ch1a. eprint: https://onlinelibrary.wiley.com/doi/pdf/10.1002/3527606696.ch1a. URL: https://onlinelibrary.wiley.com/doi/abs/10.1002/3527606696.ch1a.

[11] James Brennan-Craddock. "The investigation of a method to generate conformal lattice structures for additive manufacturing". PhD thesis. Loughborough University, 2011.

[12] V.S. Deshpande, N.A. Fleck, and M.F. Ashby. "Effective properties of the octet-truss lattice material". In: *Journal of the Mechanics and Physics of Solids* 49.8 (2001), pp. 1747–1769. ISSN: 0022-5096.

[13] Olaf Dessing et al. "Experimental study of heat dissipation in indoor sports shoes". In: *Procedia Engineering* 72 (2014), pp. 575–580.

[14] TCPoly. *Technical Data Sheet - Ice9™ Flex*. Accessed: 2023-02-25. URL: https://tcpoly.com/wp-content/uploads/2022/03/ice9_Flex_r405.pdf.

[15] Guoying Dong, Yunlong Tang, and Yaoyao Fiona Zhao. "A survey of modeling of lattice structures fabricated by additive manufacturing". In: *Journal of Mechanical Design* 139.10 (2017), p. 100906.

[16] Dheyaa SJ Al-Saedi et al. "Mechanical properties and energy absorption capability of functionally graded F2BCC lattice fabricated by SLM". In: *Materials & Design* 144 (2018), pp. 32–44.

[17] Hongshuai Lei et al. "Evaluation of compressive properties of SLM-fabricated multi-layer lattice structures by experimental test and μ-CT-based finite element analysis". In: *Mater. Des.* 169 (2019), p. 107685.

[18] Guoqi Zhang et al. "Mechanical behaviour of CFRP sandwich structures with tetrahedral lattice truss cores". In: *Composites Part B: Engineering* 43.2 (2012), pp. 471–476.

[19] Uchechukwu O Agwu et al. "Assessing Tetrahedral Lattice Parameters for Engineering Applications Through Finite Element Analysis". In: *3D Printing and Additive Manufacturing* 8.4 (2021), pp. 238–252.

[20] Young-Eun Lim, Jung-Hwan Park, and Keun Park. "Automatic design of 3D conformal lightweight structures based on a tetrahedral mesh". In: *Int. J. Precis. Eng. Manuf. - Green Technol.* 5.4 (2018), pp. 499–506.

[21] VS Deshpande, MF Ashby, and NA Fleck. "Foam topology: bending versus stretching dominated architectures". In: *Acta materialia* 49.6 (2001), pp. 1035–1040.

[22] Ajeet Kumar et al. "Energy absorption and stiffness of thin and thick-walled closed-cell 3D-printed structures fabricated from a hyperelastic soft polymer". In: *Materials* 15.7 (2022), p. 2441.

[23] Ankhy Sultana, Tsz-Ho Kwok, and Hoi Dick Ng. "Numerical assessment of directional energy performance for 3D printed midsole structures". In: *Math. Biosci. Eng.* 18.4 (2021), pp. 4429–4449.

[24] Jiawei Feng et al. "Isotropic octet-truss lattice structure design and anisotropy control strategies for implant application". In: *Materials & Design* 203 (2021), p. 109595.

[25] YH You, ST Kou, and ST Tan. "A new approach for irregular porous structure modeling based on centroidal Voronoi tessellation and B-spline". In: *Computer-Aided Design and Applications* 13.4 (2016), pp. 484–489.

[26] Guanjun Wang et al. "Design and compressive behavior of controllable irregular porous scaffolds: based on voronoi-tessellation and for additive manufacturing". In: *ACS Biomaterials Science & Engineering* 4.2 (2018), pp. 719–727.

[27] Marcus Watson, Martin Leary, and Milan Brandt. "Generative design of truss systems by the integration of topology and shape optimisation". In: *The International Journal of Advanced Manufacturing Technology* 118.3 (2022), pp. 1165–1182.

[28] Brent R Bielefeldt et al. "Development and validation of a genetic L-System programming framework for topology optimization of multifunctional structures". In: *Computers & Structures* 218 (2019), pp. 152–169.

[29] Arash Armanfar and Erkan Gunpinar. "G-Lattices: A Novel Lattice Structure and Its Generative Synthesis under Additive Manufacturing Constraints". In: *Journal of Mechanical Design* (2022), pp. 1–20.

[30] Tsz Ho Kwok. "Improving the diversity of topology-optimized designs by swarm intelligence". In: *Structural and Multidisciplinary Optimization* 65.7 (2022), p. 202.

[31] Mohamed El Bouzouiki, Ramin Sedaghati, and Ion Stiharu. "A non-uniform cellular automata framework for topology and sizing optimization of truss structures subjected to stress and displacement constraints". In: *Computers & Structures* 242 (2021), p. 106394.

[32] Valentina Tomei et al. "Structural grammar for design optimization of grid shell structures and diagrid tall buildings". In: *Automation in Construction* 143 (2022), p. 104588.

[33] Wei Huang et al. "Impulsive response of composite sandwich structure with tetrahedral truss core". In: *Composites Science and Technology* 176 (2019), pp. 17–28.

[34] Yingying Xue et al. "Experimental and Simulation Analysis on the Mechanical Behavior of 3D-Enhanced Al-Based Tetrahedral Lattice Materials". In: *physica status solidi (a)* 220.1 (2023), p. 2200580.

[35] Subramanian Senthilkannan Muthu and Yi Li. "The environmental impact of footwear and footwear materials". In: *Handbook of footwear design and manufacture* (2021), pp. 305–320.

[36] A Sasikala and A Kala. "Thermal stability and mechanical strength analysis of EVA and blend of EVA with natural rubber". In: *Materials today: Proceedings* 5.2 (2018), pp. 8862–8867.

[37] ZX Zhang et al. "A developed, eco-friendly, and flexible thermoplastic elastomeric foam from SEBS for footwear application." In: *Express Polym. Lett.* 13.11 (2019).

[38] Ali Zolfagharian et al. "Custom shoe sole design and modeling toward 3D printing". In: *International Journal of Bioprinting* 7.4 (2021).

[39] Guoying Dong, Daniel Tessier, and Yaoyao Fiona Zhao. "Design of Shoe Soles Using Lattice Structures Fabricated by Additive Manufacturing". In: *Proceedings of the Design Society: International Conference on Engineering Design* 1.1 (2019), 719–728. DOI: 10.1017/dsi.2019.76.

[40] Chongning Wang et al. "Study on Vibration Damping Mechanism of Shoe Sole with Alternating Lattice Structure Using Vibration Level Difference". In: *Mathematical Problems in Engineering* 2021 (2021).

[41] Yunlong Tang et al. "Data-driven design of customized porous lattice sole fabricated by additive manufacturing". In: *Procedia Manufacturing* 53 (2021), pp. 318–326.

[42] Mubasher Ali, Aamer Nazir, and Jeng-Ywan Jeng. "Mechanical performance of additive manufactured shoe midsole designed using variable-dimension helical springs". In: *The International Journal of Advanced Manufacturing Technology* 111.11 (2020), pp. 3273–3292.

[43] Muhammad Rizwan ul Haq et al. "Design and performance evaluation of multifunctional midsole using functionally gradient wave springs produced using multijet fusion additive manufacturing process". In: *Mater. Today Commun.* 31 (2022), p. 103505.

[44] Luis Augusto Kuwer Bugin et al. "Exploration of data-driven midsole algorithm design based in biomechanics data and Voronoi 3D to digital manufacturing." In: *Design e Tecnologia* 10.21 (2020), pp. 01–10.

[45] Yasuhiro Shimazaki and Masaaki Murata. "Effect of gait on formation of thermal environment inside footwear". In: *Appl. Ergon.* 49 (2015), pp. 55–62.

[46] Nigel AS Taylor et al. "Hands and feet: physiological insulators, radiators and evaporators". In: *European journal of applied physiology* 114.10 (2014), pp. 2037–2060.

[47] Kalev Kuklane. "Protection of feet in cold exposure". In: *Industrial Health* 47.3 (2009), pp. 242–253.

[48] Hiroshi Kinoshita and Barry T Bates. "The Effect of Environmental Temperature on the Properties of Running Shoes." In: *Journal of applied biomechanics* 12.2 (1996).

[49] M Rebay et al. "Heat transfer in athletic shoes during the running". In: *the 5th IASME/WSEAS International Conference on Heat Transfer, Thermal Engineering and Environment*. Ed. by Siavash H. Sohrab. Athens, Greece, 2007.

[50] Yasuhiro Shimazaki and Kazutoshi Aisaka. "Novel thermal analysis model of the foot-shoe sole interface during gait motion". In: *Multidisciplinary Digital Publishing Institute Proceedings* 2.6 (2018), p. 278.

[51] Kit-lun Yick, Annie Yu, and Pui-ling Li. "Insights into footwear preferences and insole design to improve thermal environment of footwear". In: *International Journal of Fashion Design, Technology and Education* 12.3 (2019), pp. 325–334.

[52] Faheem Ahmad et al. "Recent Developments in Materials and Manufacturing Techniques Used for Sports Textiles". In: *International Journal of Polymer Science* 2023 (2023).

[53] Karolyn Ning et al. "Effects of textile-fabricated insole on foot skin temperature and humidity for enhancing footwear thermal comfort". In: *Appl. Ergon.* 104 (2022), p. 103803.

[54] Christiane Beyer and Dustin Figueroa. "Design and analysis of lattice structures for additive manufacturing". In: *Journal of Manufacturing Science and Engineering* 138.12 (2016).

[55] David W Rosen, Scott R Johnston, and Marques Reed. "Design of general lattice structures for lightweight and compliance applications". In: (2006).

[56] James I Novak and Andrew R Novak. "Is additive manufacturing improving performance in Sports? A systematic review". In: *Proceedings of the Institution of Mechanical Engineers, Part P: Journal of Sports Engineering and Technology* 235.3 (2021), pp. 163–175.

[57] M. Kajtaz et al. "Chapter 5 - Three-Dimensional Printing of Sports Equipment". In: *Materials in Sports Equipment (Second Edition)*. Ed. by Aleksandar Subic. Second Edition. Woodhead Publishing Series in Composites Science and Engineering. Woodhead Publishing, 2019, pp. 161–198. ISBN: 978-0-08-102582-6. DOI: https://doi.org/10.1016/B978-0-08-102582-6.00005-8. URL: https://www.sciencedirect.com/science/article/pii/B9780081025826000058.

[58] Omar A Mohamed, Syed H Masood, and Jahar L Bhowmik. "Optimization of fused deposition modeling process parameters: a review of current research and future prospects". In: *Advances in manufacturing* 3 (2015), pp. 42–53.

[59] Guoying Dong et al. "Optimizing process parameters of fused deposition modeling by Taguchi method for the fabrication of lattice structures". In: *Additive Manufacturing* 19 (2018), pp. 62–72.

[60] Rafael Guerra Silva et al. "Manufacturing and characterization of 3D miniature polymer lattice structures using fused filament fabrication". In: *Polymers* 13.4 (2021), p. 635.

[61] Victor Beloshenko et al. "Mechanical Properties of Flexible TPU-Based 3D Printed Lattice Structures: Role of Lattice Cut Direction and Architecture". In: *Polymers* 13.17 (2021), p. 2986.

[62] KevinRoot Medical. *Foot ID*. Accessed: 2023-02-25. URL: kevinrootmedical.com/pages/foot-id-scan-app.

[63] DJ Janisse. "Pedorthic care of the diabetic foot". In: *The diabetic foot* 5 (1993), pp. 549–576.

[64] Hisham R Ashry et al. "Effectiveness of diabetic insoles to reduce foot pressures". In: *The Journal of foot and ankle surgery* 36.4 (1997), pp. 268–271.

[65] Sicco A Bus, Jan S Ulbrecht, and Peter R Cavanagh. "Pressure relief and load redistribution by custom-made insoles in diabetic patients with neuropathy and foot deformity". In: *Clinical Biomechanics* 19.6 (2004), pp. 629–638.

[66] Michael J Mueller et al. "Efficacy and mechanism of orthotic devices to unload metatarsal heads in people with diabetes and a history of plantar ulcers". In: *Physical therapy* 86.6 (2006), pp. 833–842.

[67] Si Hang. "TetGen, a Delaunay-based quality tetrahedral mesh generator". In: *ACM Trans. Math. Softw* 41.2 (2015), p. 11.

[68] Benjamin Vaissier et al. "Genetic-algorithm based framework for lattice support structure optimization in additive manufacturing". In: *Computer-Aided Design* 110 (2019), pp. 11–23. ISSN: 0010-4485. DOI: 10.1016/j.cad.2018.12.007.

[69] Juliana Felkner, Eleni Chatzi, and Toni Kotnik. "Interactive particle swarm optimization for the architectural design of truss structures". In: *2013 IEEE Symposium on Computational Intelligence for Engineering Solutions (CIES)*. IEEE. 2013, pp. 15–22.

[70] Luca Zimmermann, Tian Chen, and Kristina Shea. "A 3D, performance-driven generative design framework: automating the link from a 3D spatial grammar interpreter to structural finite element analysis and stochastic optimization". In: *AI EDAM* 32.2 (2018), pp. 189–199.

[71] Yicha Zhang et al. "Bio-inspired generative design for support structure generation and optimization in Additive Manufacturing (AM)". In: *CIRP Annals* 69.1 (2020), pp. 117–120.

[72] Russell C Eberhart, Yuhui Shi, and James Kennedy. *Swarm intelligence*. Elsevier, 2001.

[73] Carlos A Coello Coello, Gregorio Toscano Pulido, and Maximino Salazar Lechuga. "Handling multiple objectives with particle swarm optimization". In: *IEEE Transactions on evolutionary computation* 8.3 (2004), pp. 256–279.

[74] S Killi and A Morrison. "Fea and 3D printing, the perfect match". In: *International Journal of Mechanical Systems Engineering* 2.1 (2016), p. 7.

[75] Elena Provaggi et al. "3D printing assisted finite element analysis for optimising the manufacturing parameters of a lumbar fusion cage". In: *Materials & Design* 163 (2019), p. 107540.

[76] Hassan Gonabadi et al. "Investigation of the effect of raster angle, build orientation, and infill density on the elastic response of 3D printed parts using finite element microstructural modeling and homogenization techniques". In: *The international journal of advanced manufacturing technology* (2022), pp. 1–26.

[77] Vidya K Nandikolla et al. "Experimental gait analysis to study stress distribution of the human foot". In: *Journal of medical engineering* 2017 (2017).

[78] J Martin Bland and Douglas G Altman. "Statistics notes: Measurement error". In: *BMJ* 312.7047 (1996), p. 1654. DOI: 10.1136/bmj.312.7047.1654.

[79] L. Jones. "Thermal touch". In: *Scholarpedia* 4.5 (2009). revision #150165, p. 7955. DOI: 10.4249/scholarpedia.7955.

[80] M Matlack et al. "Investigation of Ultem 1010 FDM sparse-build parts using design of experiments and numerical simulation". In: (2016).

[81] Caterina Casavola et al. "Orthotropic mechanical properties of fused deposition modelling parts described by classical laminate theory". In: *Materials & design* 90 (2016), pp. 453–458.